NIST-GCR-90-581

AN INVESTIGATION OF SIMULATED OIL-WELL BLOWOUT FIRES

J. P. Gore
S. M. Skinner
U. S. Ip

University of Maryland
Department of Mechanical Engineering
College Park, MD 20742

Sponsored by:
U.S. DEPARTMENT OF COMMERCE
National Institute of Standards
and Technology
National Engineering Laboratory
Center for Fire Research
Gaithersburg, MD 20899

U.S. DEPARTMENT OF COMMERCE
Robert A. Mosbacher, Secretary

NATIONAL INSTITUTE OF STANDARDS
AND TECHNOLOGY
John W. Lyons, Director

NIST

NIST-GCR-90-581

AN INVESTIGATION OF SIMULATED OIL-WELL BLOWOUT FIRES

J. P. Gore
S. M. Skinner
U. S. Ip

University of Maryland
Department of Mechanical Engineering
College Park, MD 20742

Annual Report
September 1990

Issued November 1990
NIST Grant No. 60NANB8D0834

Sponsored by:
U.S. DEPARTMENT OF COMMERCE
National Institute of Standards
and Technology
National Engineering Laboratory
Center for Fire Research
Gaithersburg, MD 20899

U.S. DEPARTMENT OF COMMERCE
Robert A. Mosbacher, Secretary

NATIONAL INSTITUTE OF STANDARDS
AND TECHNOLOGY
John W. Lyons, Director

Notice

This report was prepared for the Center for Fire Research of the National Institute of Standards and Technology under Grant Number 60NANB8OD0834. The statements and conclusions contained in this report are those of the authors and do not necessarily reflect the views of the National Institute of Standards and Technology or the Center for Fire Research.

AN INVESTIGATION OF SIMULATED OIL-WELL BLOWOUT FIRES

J. P. Gore, S. M. Skinner and U. S. Ip
The University of Maryland
Mechanical Engineering Department
College Park, MD 20742

Annual Report for Grant No. 60NANB8D0834

September 1989

Prepared for

U. S. Department of Commerce
National Institute of Standards and Technology
Center for Fire Research
Gaithersburg, MD 20899.

ABSTRACT

A study of simulated oil well blowout fires aimed at improving the predictive capabilities needed for the development of radiation and fire suppression technology is described. Measurements of temperature distributions and radiative heat flux to representative locations are used to evaluate the analysis. Methane/air flames with suppression and heptane+methane/air flames without suppression are considered. The analysis consists of (i) construction of state relationships for fuel with water addition and two phase fuel mixtures using species concentration data for single fuels with the help of mixing rules and (ii) application of an existing flow solver under the locally homogeneous flow approximation. The predictions and measurements are in reasonably good agreement. Direct verification of the mixing rule for state relationships and treatment of two phase flow effects is necessary for further improvement.

ACKNOWLEDGEMENT

This research was sponsored by the United States Department of Commerce, National Institute of Standards and Technology, Center for Fire Research, Gaithersburg, MD 20899, with Dr. D. D. Evans serving as Scientific Officer. The large scale experiments were performed at the Center for Fire Research under a grant from the Mineral Management Service of the United States Department of Interior by Mr. Dave Stroup and Mr. Dan Madrzykowski with Dr. D. D. Evans serving as the Principal Investigator and Mr. Ed Tennyson of MMS serving as the Scientific Officer.

TABLE OF CONTENTS

LIST OF FIGURES

LIST OF FIGURES (CONTINUED)

NOMENCLATURE

d	burner exit diameter
f	mixture fraction
g	square of mixture fraction fluctuations
H	total enthalpy(Chemical+ Sensible)
h^o_{fi}	heat of formation of species i
Δh_i	sensible energy of species i
k	turbulent kinetic energy
m	burner mass flow rate
N	number of product species
Q	chemical energy release
Re	burner exit Reynolds number
Ri	burner exit Richardson number
T	temperature
u	streamwise velocity
u_o exit	equivalent streamwise velocity at the burner
x	height above the burner
X_r	radiative heat loss fraction
Y_i	mass fraction of species i
ϵ energy	rate of dissipation of turbulence kinetic

1. INTRODUCTION

The Mineral Management Service of the U. S. Department of Interior has sponsored a comprehensive research program concerning the development of suppression technology for oil well blowout fires at the Center for Fire Research, National Institute of Standards and Technology, U. S. Department of Commerce. The present investigation is a part of the overall program aimed at developing analyses capable of scaling results from controlled simulations of oil well blowout fires to practical sizes. The results of the research have applications to fire suppression and thermal radiation control technologies for offshore oil well platforms. The generic findings also have applications to modeling fires within structures and for design of suppression technology, safe egress times and hazard prediction.

Past studies (Evans and Pfenning, 1985; McCaffrey, 1984, 1986 (also 1989), McCaffery and Evans, 1986; Gore et al., 1986; and Pfenning, 1985) have simulated oil well blowout fires as a release and non-premixed combustion of high pressure gaseous fuels(primarily methane) from a large reservoir. Effects of adding water as a suppressant have been studied experimentally. However, detailed theoretical analyses have been restricted to flames without suppression. Past studies have also been restricted to gaseous fuels while the effluent of an oil well blowout consists of both gaseous and liquid hydrocarbons. The objective of the present study is to investigate the flame

structure and radiation properties of single and two phase non-premixed flames burning liquid and gaseous fuels with and without water suppression.

Work during the first year of this grant is divided into three parts: (1) Effects of water addition on the structure and radiation properties of natural gas flames , (2) Structure and radiation properties of flames burning two phase fuel mixtures and (3) Construction of a laminar flame burner for insitu measurements of state relationships in fuel mixtures and measurements of soot volume fractions in laminar flames (burning mixtures of acetylene and methane) stabilized on this burner.

The laminar flamelet concept and the locally homogeneous approximation (Faeth, 1988) are utilized in the first two parts of the study. Approximate state relationships for fuel-water mixtures and two-fuel mixtures are obtained from measurements of gas concentrations in laminar flames burning single fuels. Once the state relationships are known, the calculations follow the existing procedure for flame structure and radiation analyses.

A laminar coflow burner is constructed in order to evaluate the approximate state relationships using measurements of gas species concentrations and soot volume fractions. The soot volume fraction measurements are completed and the gas concentration measurements are about to begin as a part of the continuation of the present grant.

The effects of liquid water suppressant are assumed to be purely thermal (Seshadri, 1978). Under this approximation, the state relationships for species concentrations in methane and water flames (with water sprayed into the fuel stream) are constructed using the measurements of gas species concentrations in laminar flames burning methane without the water spray. This approach may not be valid for sooty fuels since soot concentrations are known to decrease significantly with the addition of water. The radiative heat loss fractions of flames burning fuel-water mixtures depend on the water content and are not known apriori. Predictions of temperature and radiative heat flux for methane flames with and without water addition are completed using the above methods and compared with experimental data of McCaffrey (1986 (also 1989)).

Consideration of a mixture of two fuels within the laminar flamelet concept requires the construction of state relationships for a mixture. These state relationships can be obtained from laminar flames burning the different fuel mixtures. However, in the absence of a mixing rule, separate measurements for all the possible combinations of mass ratios between the two fuels would be required. Treatment of mixtures of liquid and gaseous fuels introduces inherent separation between the fuel components that is conceptually beyond the single fuel state relationship concept. In the present, the Locally Homogeneous Flow (LHF) approximation of two phase flow theory (Faeth, 1988) is applied

to treat the multiphase aspects. A heuristic mixing rule for state relationships of different fuel components was used to treat the multifuel aspects of the problem. The construction of state relationships for temperature and density is somewhat complicated by changes in the radiative heat loss fractions that are not known apriori. Measurements of radiative heat loss fractions for flames burning mixtures of fuels are currently in progress.

In the following, progress made in the three parts of the project is described separately. The plans for ongoing research concerning oil well blowout and diverter fires.

2. EFFECTS OF WATER ADDITION ON FLAME STRUCTURE AND RADIATION

McCaffrey (1986 (also 1989)) conducted measurements of temperature profiles and radiative heat fluxes to the surroundings for methane flames in the heat release range (1MW-10 MW) with and without injection of controlled amounts of liquid water. In this study these data are used to evaluate the present analysis. The tests were started with pure methane and then the injection of water from within the fuel tube was started. This allows comparison of the baseline methane flames without the action of water. In the following the tests are summarized briefly followed by a discussion of the analysis and finally the results of the analysis are compared with the data.

2.1 Description of the Experiments

The experimental apparatus used by McCaffrey (1986 (also 1989)) involved a 104 mm diameter main natural gas pipe with a pressure atomizing nozzle (PAN) mounted at the center at a depth of 59 mm from the exit as shown in Figure 1. At the exit the pipe had a sudden contraction to 32 mm diameter. The twin fluid pressure atomizing nozzle was supplied with liquid water in the central portion and atomizing methane (called "Driver" by McCaffrey (1986 (also 1989)) in the annulus. The atomizing methane was admitted at approximately 150 KPa. Two different exit geometries were considered (sharp-edged orifice or straight cut hole). However, the differences in the measurements were within the measurement uncertainties. The nozzle was located at the bottom of a 5 m deep underground pit. Air entered the pit from large openings at the surface.

Water and atomizing methane were metered using rotometers. The main methane flow was metered using a laminar flow element. The temperature measurements involved six chromel - alumel thermocouple junctions formed from 0.5 mm diameter wire mounted at 0.5, 1, 2, 3, 4 and 5 meters from the injector exit. The radiative heat flux detectors involved two wide angle (150^{o} view angle) broad band radiometers (Medtherm Corp.) mounted at: (1) 2.6 m radius and 1.9 meters height from the injector exit and (2) 3.5 m radius and 2.5 meters height from the injector exit. The

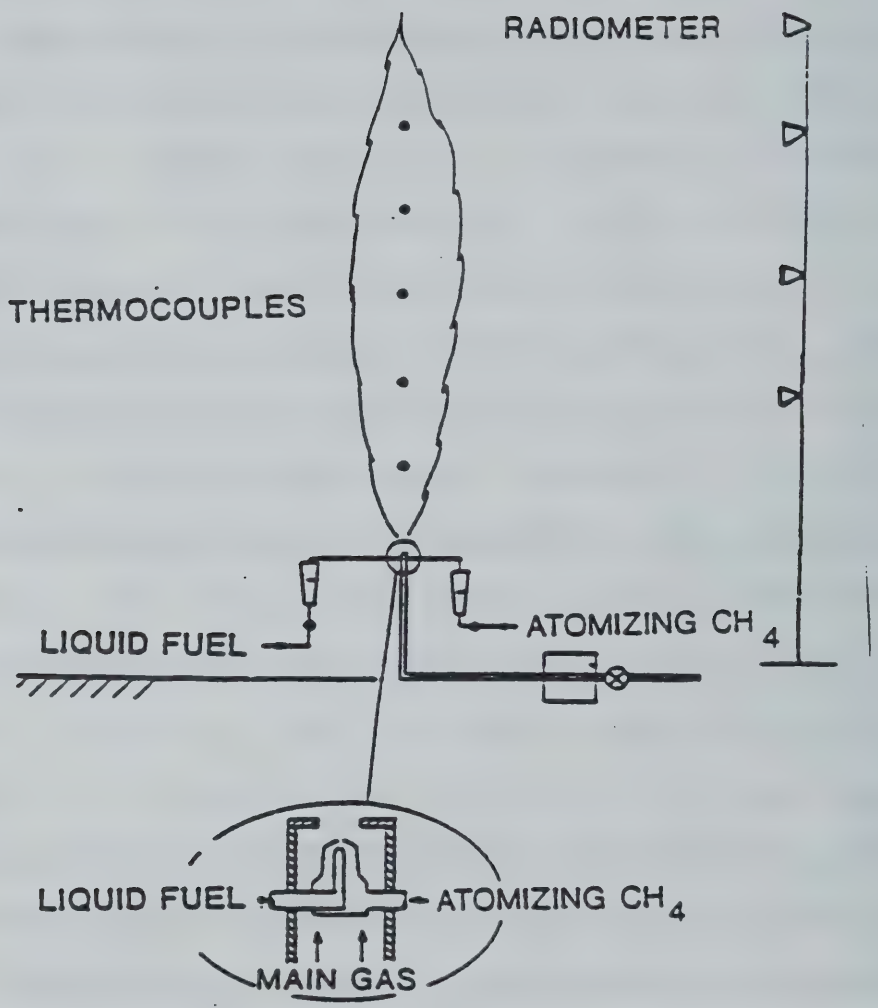

Figure 1. Sketch of the Experimental Apparatus.

radiometer locations were selected to sample representative radiative heat flux distribution around the flames.

The nominal heat release rates for the operating conditions selected by McCaffrey (1986 (also 1989)) varied between 1-10 MW. These conditions yield fully turbulent (exit Reynolds numbers 30,000 - 500,000) flow at the jet exit. The flames are momentum dominated in the near-injector region but buoyancy influences the flame height due to reduction in local momentum of the jets by mixing. According to the criterion of Becker and Liang(1978), the flames are in the intermediate regime (Ri = 0.000014 - 0.00012). Many of the flames were lifted from the injector exit since no pilots or other methods of flame attachment were provided.

The tests were begun by first lighting a small pilot flame of methane and then increasing the fuel mass flow until the desired operating condition was reached. During the extinction tests, two minutes after the establishment of the desired gas flow condition, the water flow was started and increased in desired steps until the limiting flow was reached. This allowed collection of temperature profile data and radiative heat flux data for the baseline methane flames without water suppression and also data for flames with different water/methane mass ratios.

2.2 Theoretical Methods

Since radiation for methane flames is dominated by gaseous bands, effects of water addition are assumed to be purely thermal Seshadri(1978). Thus the state relationships for flames with water added to the fuel stream are constructed using species concentration data for flames burning methane and adding liquid water to the fuel in an appropriate amount as an inert species. The effect of water is to reduce the temperatures by extracting the heat of vaporization and sensible heat from the material.

It is also assumed that the water is added to the fuel stream in the form of very fine droplets so that the instantaneous velocities of the two phases are identical at the exit and that the differential diffusion effects between the gas phase and water drops are negligible. This corresponds to the locally homogeneous flow (LHF) approximation described by Faeth (1977, 1983 and 1988).

The density of the material leaving the injector is increased due to the presence of liquid water reducing the air entrainment rates for the jet. The velocity of the jet leaving the injector is calculated using mass balance and assumed to be uniform at the jet exit. In addition to initial density and velocity distributions, mixture fraction, turbulence kinetic energy, mixture fraction fluctuations and dissipation of turbulence kinetic energy are needed at the initial station. Approximate initial conditions are specified similar to past practice (Gore et al, 1986 and Faeth, 1988). Once the

distributions of the above variables in the flow are known, mean scalar properties needed for calculating radiative heat flux such as temperature and species concentrations are obtained from the state relationships using averaging based on a clipped Gaussian probability density function (Jeng and Faeth, 1984).

State Relationships in the Presence of Liquid Water

Measurements of gaseous species concentrations for laminar flames burning methane in air (Tsuji and Yamaoka, 1969) show that the global reaction (considering only the species whose mole fractions are above 0.01 as important for the present radiation calculations) can be written as:

$$aCH_4 + b\ O_2 + 3.76\ b\ N_2 = x_{CH_4}\ CH_4 + x_{N_2}\ N_2 + x_{CO_2}\ CO_2 + x_{H_2O}\ H_2O + x_{CO}\ CO + x_{H_2}\ H_2 \qquad (1)$$

Where "x_i" indicates the mole fraction of product species "i" and "a" and "b" are determined by atom balances. In order to construct the state relationships for methane with liquid water burning with air, x_w moles of liquid water are added to the fuel stream per mole of liquid water. Since the results of this addition are only thermal, the chemical reaction now becomes:

$$aCH_4 + ax_w\ H_2O\ (l) + b\ O_2 + 3.76b\ N_2 = x_{CH_4}\ CH_4 + x_{N_2}\ N_2 + x_{CO_2}\ CO_2 + cx_{H_2O}\ H_2O\ (v) + dx_{H_2O}\ H_2O\ (l) + x_{CO}\ CO + x_{H_2}\ H_2 \qquad (2)$$

where the product side no longer contains 1 mole as was the case in equation (1) and therefore x_i now are the actual moles of

product species "i" in reaction represented by Eq. (2). The moles of water added per mole of CH_4 are calculated from the operating conditions. The additional unknown in Eq. (2) is the moles of water in the liquid form in the products. Under the present approximations the mole fraction of water vapor must satisfy the equilibrium partial pressure value based on the vapor pressure relationship. Thus the mole fraction of water in the vapor phase is:

$$x_{H_2O}\ (v) = P_v\ (T) \tag{3}$$

Temperature of the products must be known to find the vapor pressure using Eq. (3). The temperature is obtained using the first law of thermodynamics with a fixed radiative heat loss fraction X_R for a given water addition. This can be summarized as:

$$(1-X_R)\ (\sum x_i h^o_{fi\ R} - \sum x_i h^o_{fi\ P}) = \sum x_i h_{i\ P} \tag{4}$$

Eq. (3) and (4) must be solved simultaneously for obtaining the partial pressure of water vapor and the temperature of the products. The mole fractions of individual product species are then obtained using atom balance on Eq. (2).

The density of the two phase mixture is obtained noting that the specific volumes of the two phases are additive:

$$v = Y_g\ v_g + Y_l\ v_l \tag{5}$$

where v is the specific volume of the mixture and Y_g is the mass

fraction of all species in the gas or vapor phase (specific volume v_g) and Y_l is the mass fraction of the liquid water (specific volume v_l).

The mixture fraction of each point in the state relationship for a fuel water mixture is calculated by modifying the mixture fractions in the gaseous fuel state relationship to include the effect of water addition:

$$f_l = f(x_w W_w / W_{CH_4} + 1) \; / \; (1 + f x_w W_w / W_{CH_4}) \qquad (6)$$

The gas phase mole fractions of all the species are affected due to the addition of water. These are calculated by renormalizing the RHS of Eq. (2). Thus the mole fraction of water vapor at all mixture fractions increases due to water addition while the mole fractions of all other gaseous species decrease.

2.3 Results and Discussion:

Flames without Water Addition

As discussed before, the experimental procedure allowed the collection of data for flames burning methane without the addition of water suppressant as a baseline. In the following, these data are used to compare the baseline predictions first before considering the effects of water addition. Present theoretical methods have been evaluated in the past for laboratory flames (around 20 kW heat release, Jeng and Faeth, 1984) and very large scale flames (around 200 MW heat release,

Gore et al., 1986). The present tests allow an evaluation of the scaling effects using intermediate size flames (heat release rates between 1 - 10 MW).

Figure 2 shows measurements and predictions of temperature along the axis of a 4.6 MW flame burning methane without water suppressant. The symbols represent averages of data from several runs. The data are not corrected for radiation heat loss from the thermocouples. The predictions are in reasonable agreement with the data considering limitations of the present analysis, measurement uncertainty and effects of flame liftoff. The agreement between data and predictions is similar to earlier performance of the analysis.

Radiative heat flux measured by two radiometers facing the axis of the flames are plotted in Figure 3. The radiometer positions are arbitrary and therefore representative of the surrounding locations. The positions utilized by McCaffrey (1986 (also 1989)) are given in the inset of Figure 3. Predictions of the radiative heat flux using the discrete transfer method are also plotted in Figure 3. The radiative heat flux is plotted as a function of the nominal heat release rate of the flames. As seen from Figure 3, the agreement between predictions and measurements is good for the range (0.5 - 7 M) of heat release rates considered. The slope of the heat flux versus heat release rate curves changes due to the flame length and width variations introduced by the effects of buoyancy and momentum (characterized

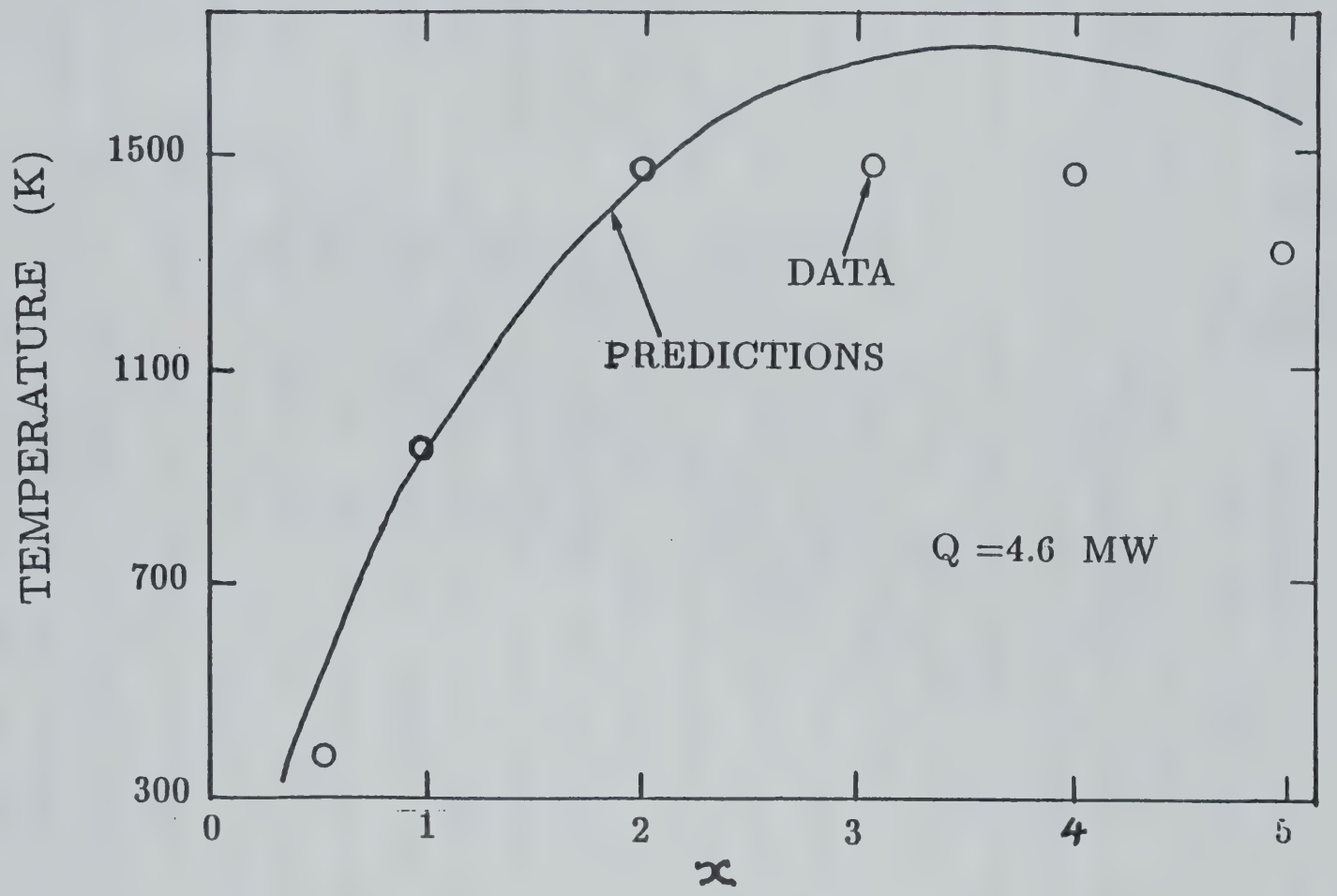

Figure 2. Temperature Distribution along the Axis of 4.6 MW Methane Flames.

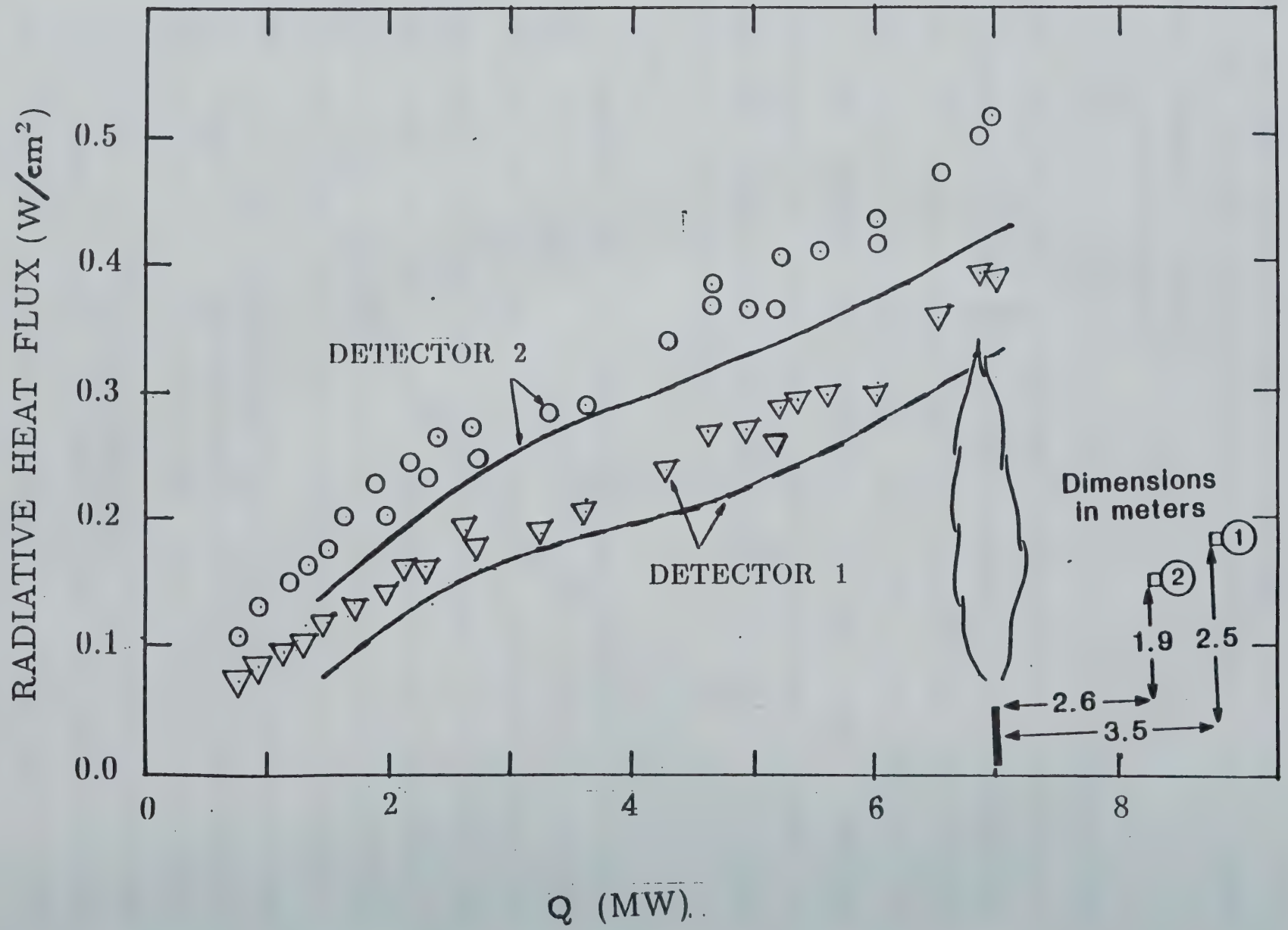

Figure 3. Radiative Heat Flux as a Function of Heat Release Rate for Methane Flames in the Range 0.5 MW to 8 MW.

by the Richardson number). It is particularly encouraging that the analysis captures the changes in the slope observed from the data.

Effect of Water Addition on State Relationships

The effects of water addition on the state relationships are described next. Figure 4 is a plot of mole fractions of water vapor as a function of equivalence ratio (which is a single valued function of mixture fraction) for no water addition and for four water mass loading ratios (m_{H_2O}/mCH_4). For all the water loadings shown in Figure 4, the water vapor mole fractions are higher than the baseline case. At a water loading ratio of 3, the peak mole fraction of water vapor is over 0.4 at an equivalence ratio of 2 . The peak occurs on the fuel rich side because the liquid water is added to the fuel and the contribution from its vaporization is much higher for this loading ratio than the contribution from the oxidation of methane. The water vapor mole fraction decreases sharply for equivalence ratios greater than 2.0 since the additional water remains in the liquid form due to lower temperatures attained by evaporation as discussed later on. For a water loading ratio of 2.0, the peak water vapor mole fractions occur at an equivalence ratio of 3.0. As the water loading is decreased further, the state relationships develop two peaks- one corresponding to the stoichiometric point and another corresponding to the maximum vapor phase equilibrium mixture. In fact at a water loading ratio of 0.46, the water vapor mole fraction is highest at an equivalence ratio of 10.

The mole fractions of water vapor have an effect on the

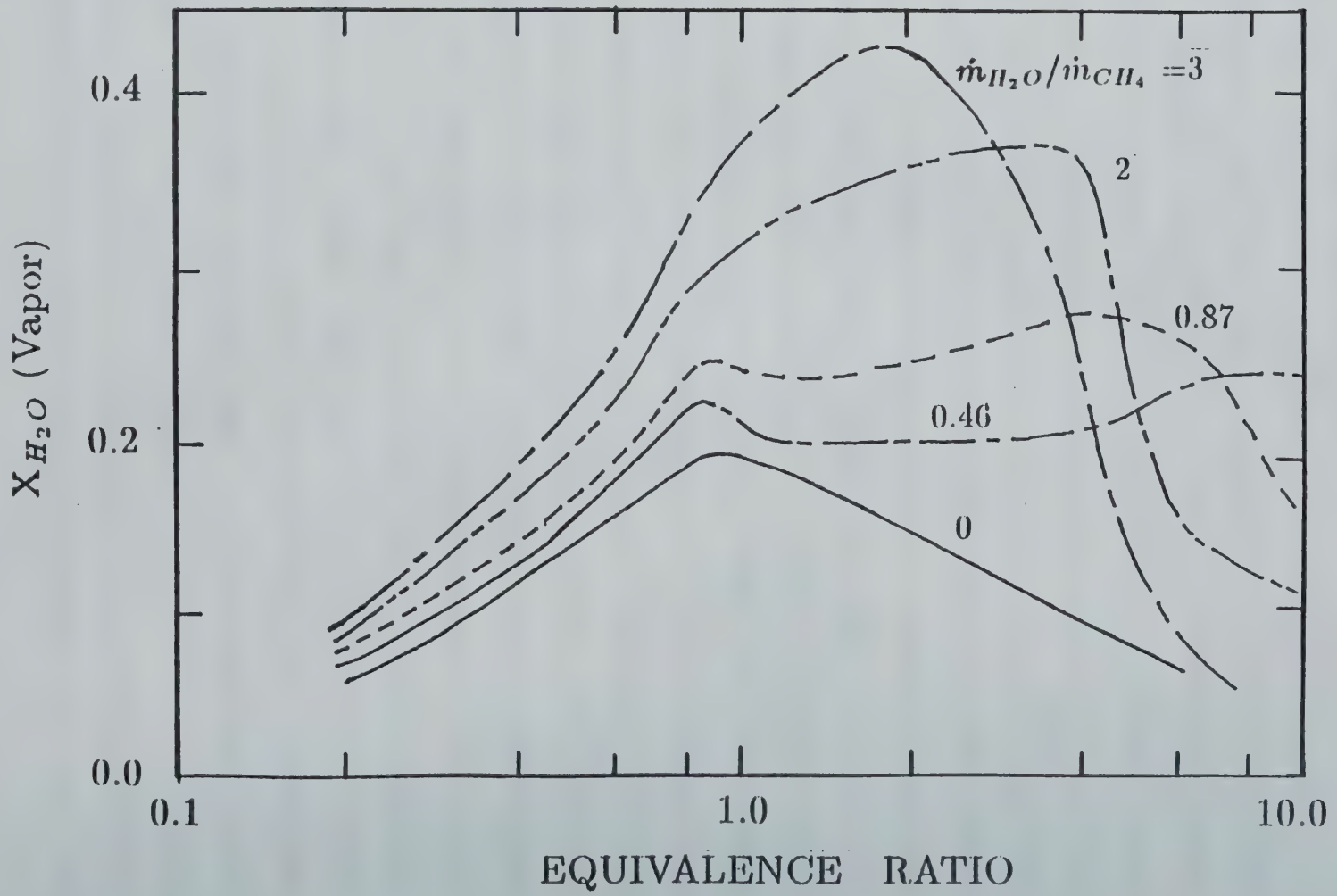

Figure 4. State Relationships for Water Vapor Mole Fraction for Methane Flames with Water Suppressant.

absorption coefficient in the water vapor bands as discussed by McCaffrey (1986 (also 1989)). However, the overall absorption coefficient also depends on the concentrations of CO_2 and on temperature and may vary in a complicated way as water loading is increased.

The state relationships for the mole fractions of liquid water are plotted in Figure 5. These show maximum liquid water at the highest fuel equivalence ratio (10 in Figure 5) for all water loadings. The liquid water mole fraction decreases as the equivalence ratio decreases for all loadings. The rate of decrease is lower for relatively rich mixtures, but increases rapidly at an equivalence ratio that decreases with increasing water loading. Figure 5 shows that liquid water reaches nearer the stoichiometric flame surface as the water loading is increased. It appears that at a loading ratio between 2 to 3, liquid water penetrates the active reaction zone explaining the critical loading for flame extinction. As liquid water penetrates to locations near the flame surface, the heat loss from the flame to the fuel side (when water is added to the fuel stream) increases continuously. At water loadings near extinction the heat loss would be such that chemical reactions can no longer be sustained. The enhanced heat loss can be studied using the temperature state relationships discussed in the following.

Figure 6 shows the state relationships for temperature. The radiative heat loss fraction is assumed to be constant at 0.18 in calculating these state relationships. Thus the coupling between

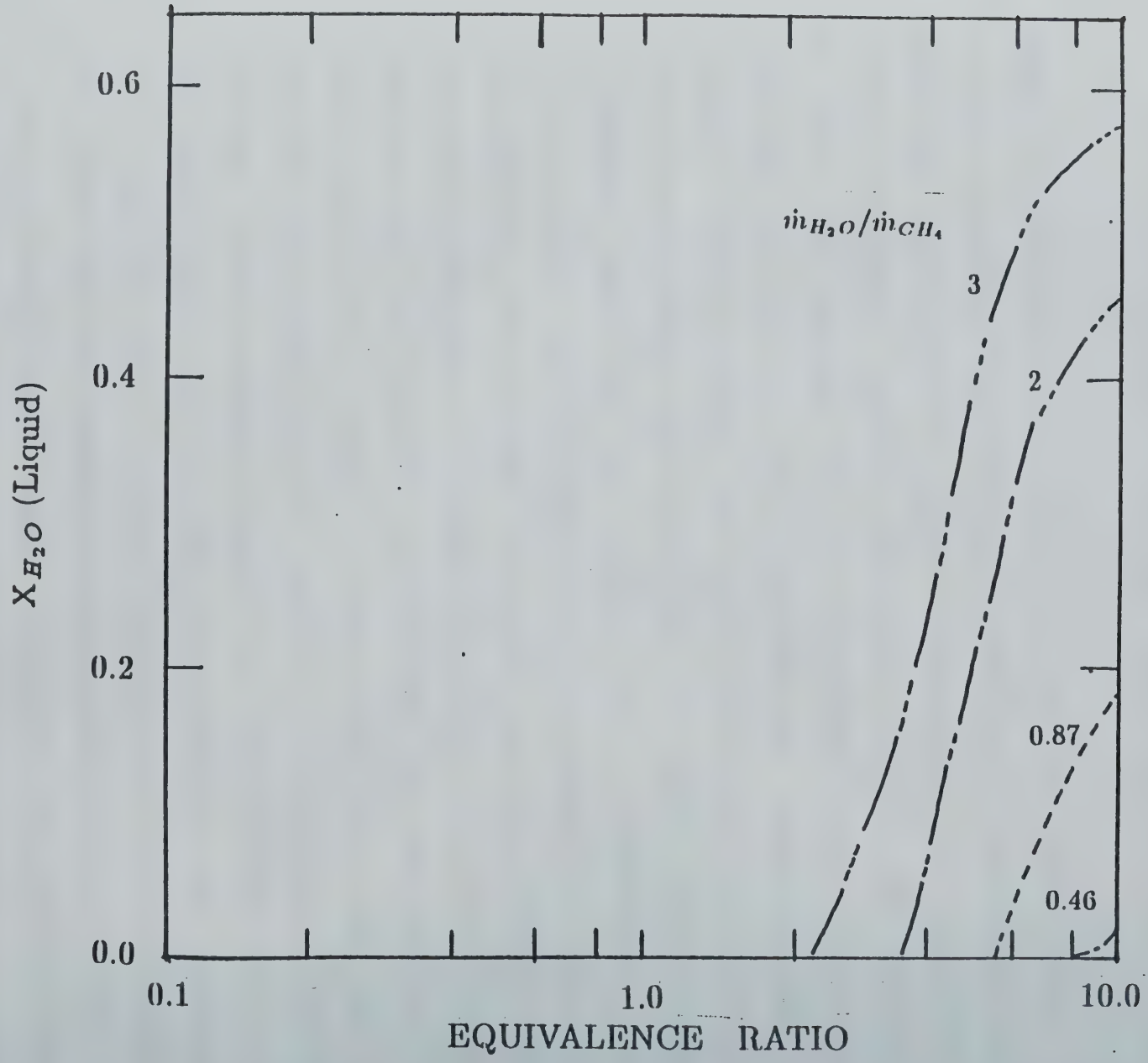

Figure 5. State Relationships for Liquid Water Mole Fraction for Methane Flames with Water Suppressant.

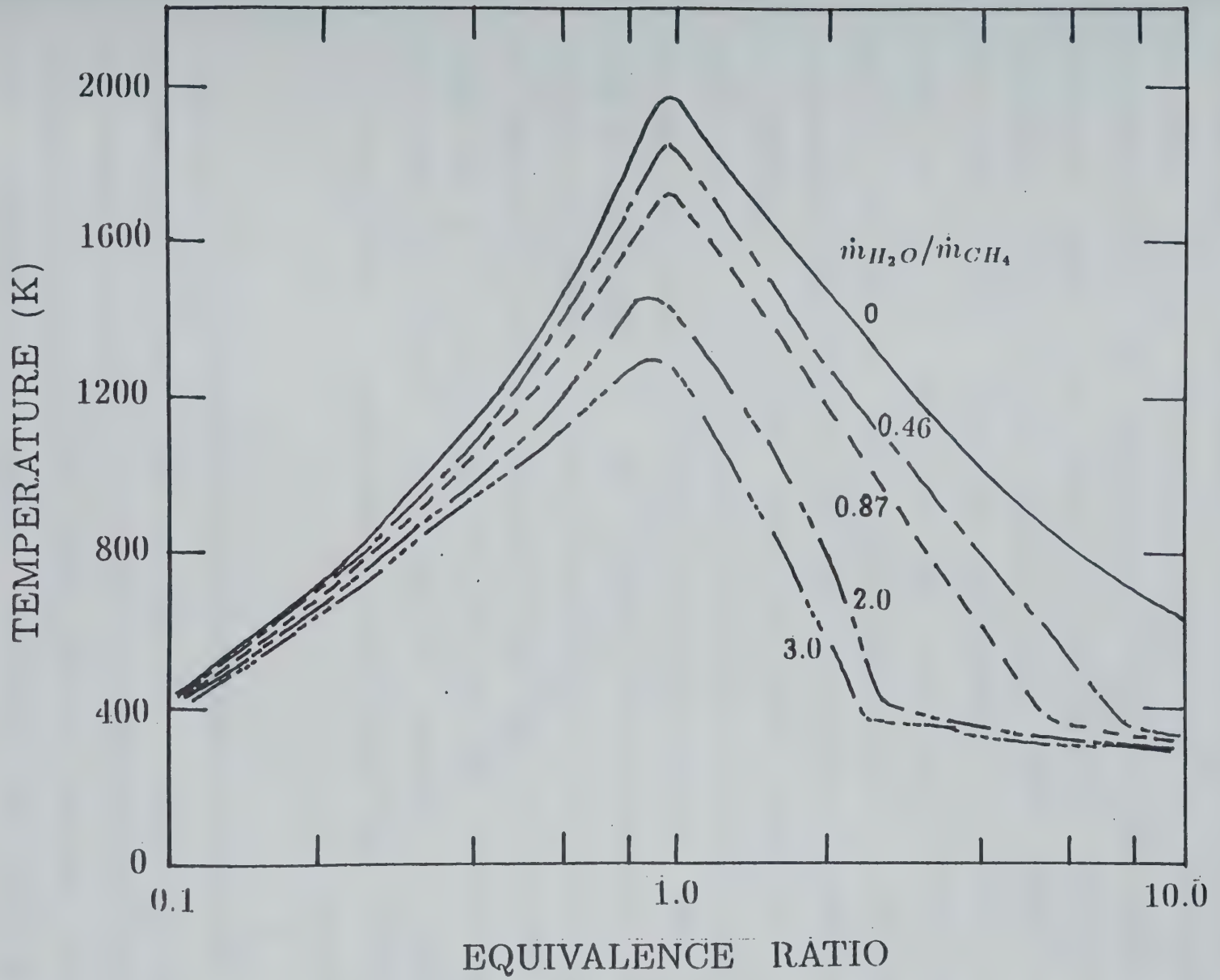

Figure 6. State Relationships for Temperature for Methane Flames with Water Suppressant.

radiative heat losses and the flow enthalpy has been neglected similar to past practice. The state relationships for temperature without water addition show a peak temperature of approximately 2000 K near the stoichiometric point. As the water loading is increased, the peak temperature decreases. At low water loadings, all the water is evaporated in the very rich regions. In regions where liquid water exists, the temperature is held to relatively low values as dictated by the vapor pressure curve. At equivalence ratios leaner than the point at which all water evaporates, the temperature rises rapidly up to the stoichiometric equivalence ratio of unity and then decreases on the fuel lean side. The peak temperature decreases to approximately 1400 K at a water loading ratio of 2 and to 1300 K at a water loading ratio of 3. These temperatures are close to where the rates of most chemical reactions are reduced to such small values that in the presence of heat loss extinction occurs. The rate of heat loss can be assessed based on the gradient of temperature at the peak. As seen from Figure 6, as the water loading is increased, the heat loss to the fuel rich side increases significantly while the heat loss to the fuel lean side decreases only slightly.

The effect of water addition on the mole fractions of CO_2 is plotted in Figure 7. Two representative water loadings together with the baseline zero water loading case are shown. As seen from Figure 7, the mole fraction of CO_2 decreases for all equivalence ratios as the water loading is increased. Thus although the flame

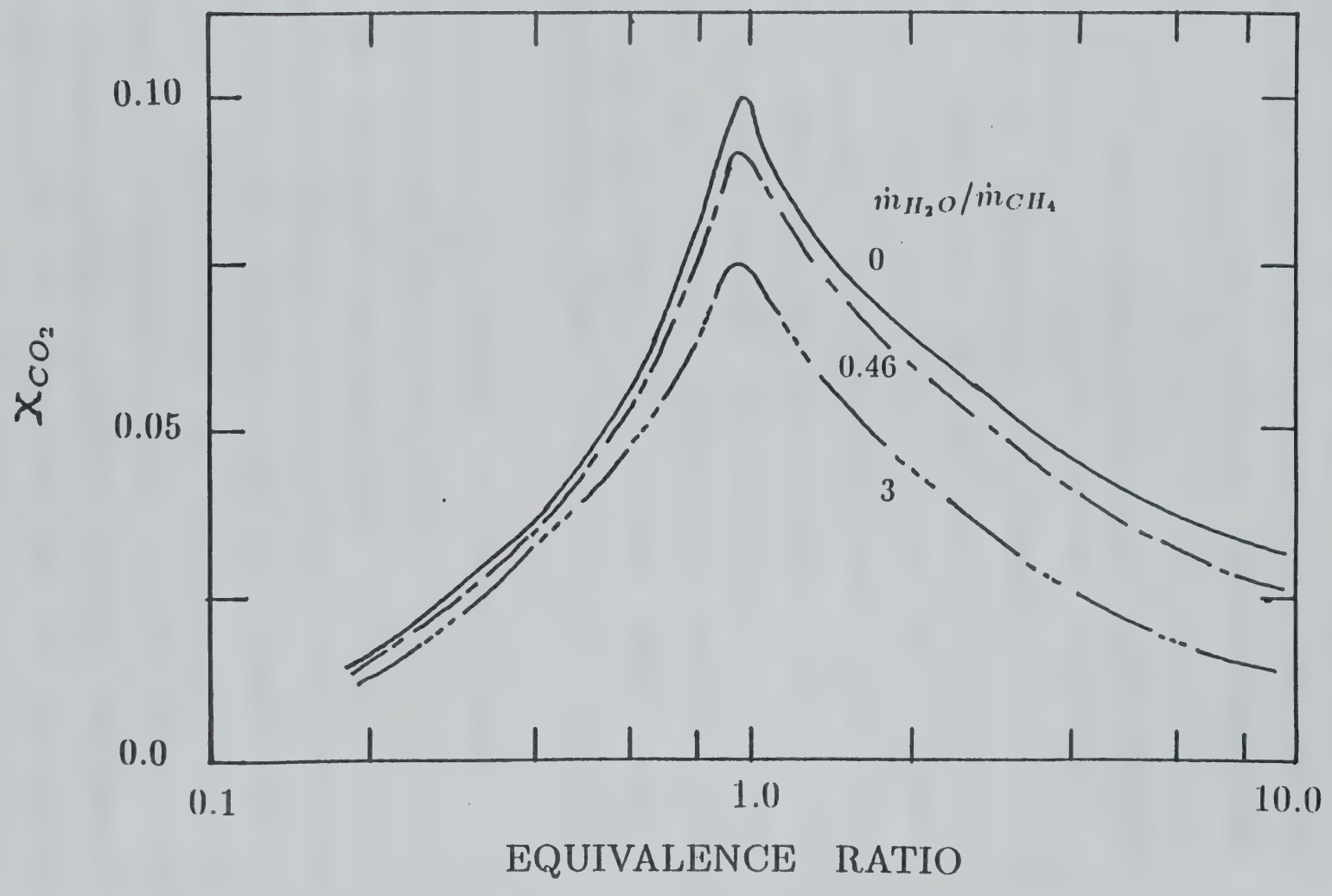

Figure 7. State Relationships for CO_2 Mole Fractions for Methane Flames with Water Suppressant.

absorption coefficient would increase due to additional water vapor, it would decrease due to a reduction in CO_2 mole fraction. The net effect is not trivial since the absorption coefficient is also a function of temperature.

Effect of Water Addition on Turbulent Flames

The effect of water addition on the turbulent flames is studied by examining the measurements and predictions of temperature at 4 meters from the injector exit (a representative location) for the 4.6 MW flame. This location remains approximately the position of the peak temperature based on both the data and the predictions. This is a combined effect of the reduced air requirements for complete combustion, increased initial momentum and decreased buoyancy on air entrainment with increased water loading. It is encouraging that the analysis predicts the combined effect of these complex phenomena.

Figure 8 shows the variation in the temperature as a function of water loading. The difference between measurements and predictions is approximately 400 K for zero water loading. As the water loading increases, the predicted temperature decreases somewhat faster than the measurements such that the difference between the measurements and the predictions is reduced to less than 100 K. Thus the reduction temperature is overpredicted by the analysis. This is probably due to the assumption of complete evaporation in the analysis. In the experiment complete evaporation was not realized due to imperfect atomization. A

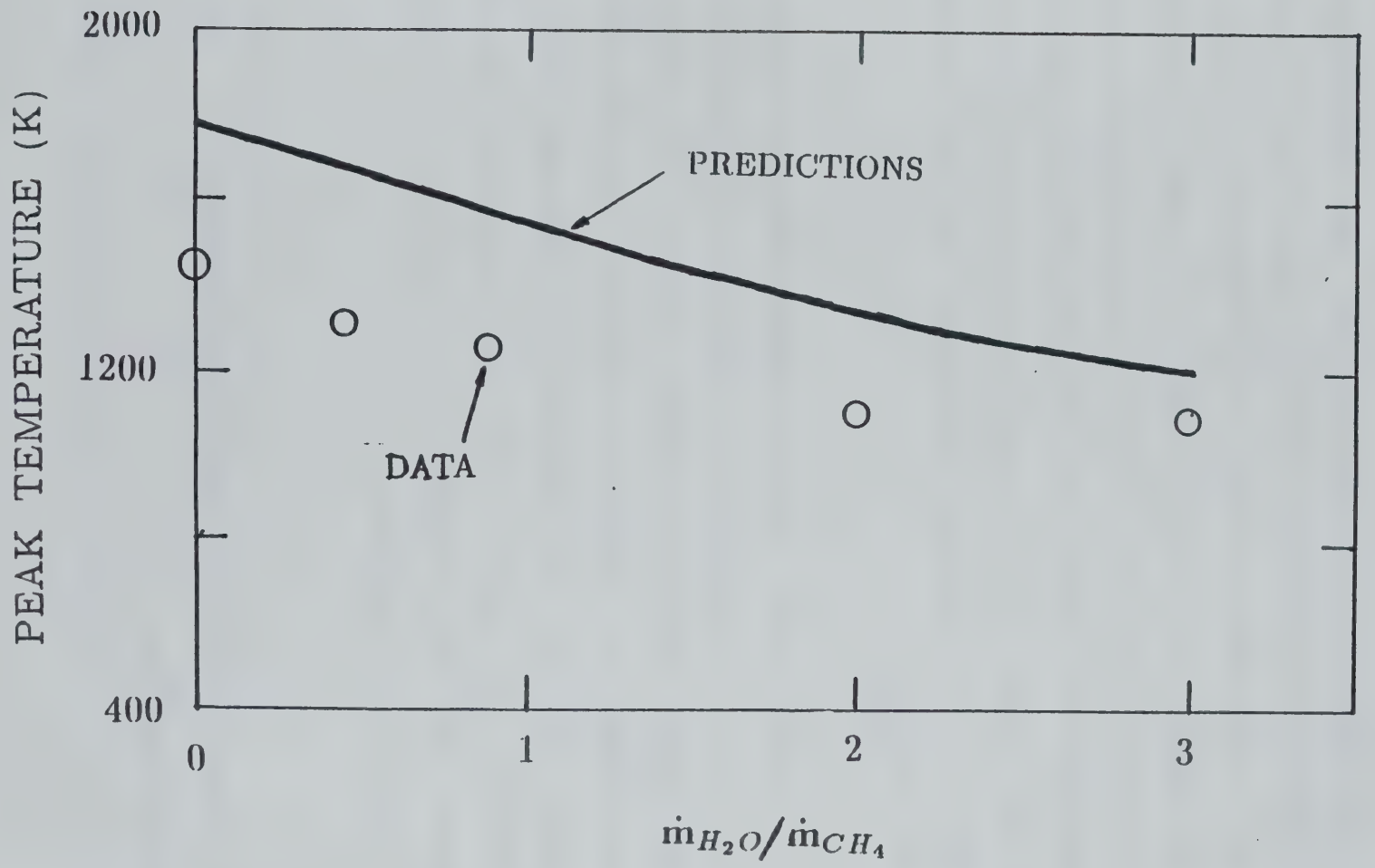

Figure 8. Peak Temperature as a Function of Water Loading for Turbulent Methane Flames with Water Suppressant.

second reason for the increased temperature drop is associated with the reduced radiative heat losses that are not considered in the construction of the temperature state relationships. However, this effect was found to be small based on a parametric analysis of the radiation calculations. Thus the discrepancies appear to be associated with the incomplete evaporation of water within the spray. This effect can only be addressed by considering separated flow models with finite evaporation rates. The temperature of the flames with water addition appears to be underestimated in comparison to flames with out water addition based on Figure 8. If the temperature is truly underestimated, the radiative heat flux to surrounding locations is also expected to be underestimated.

Figure 9 shows the measurements and predictions of radiative heat flux at a representative location as a function of the water loading. As the water loading increases the difference between measurements and predictions increases progressively. At a water loading of 0.5, the decrease in radiative flux is predicted correctly. It appears that the temperature is underestimated because of the assumption of complete evaporation of water leading to this difficulty.

3. FLAMES BURNING TWO PHASE FUEL MIXTURES

3.1 Introduction

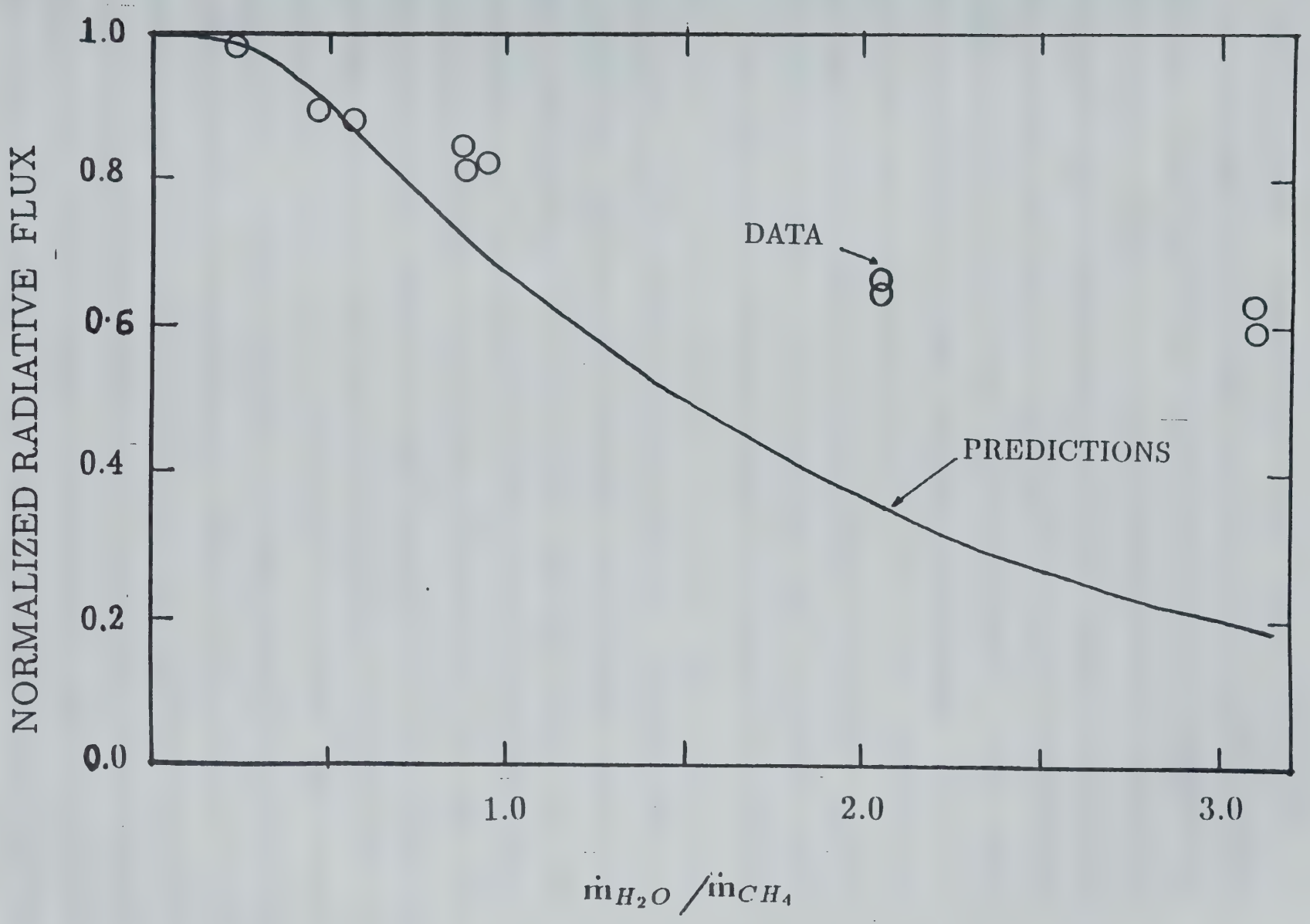

Figure 9. Radiative Heat Flux for Methane Flames with Water Suppressant.

Faeth (1977, 1983, 1988) has reviewed current analyses of combusting sprays. Past work has generally been restricted to the consideration of liquid sprays injected into combustion environments with pressure- or air- atomization. Radiation from such spray flames has been considered using multiflux approximations by some investigators (Gosman and Ioannides,1981; Gosman et al., 1980; Swithenbank et al., 1980; Mongia and Smith, 1979) while neglected by others(El Banhawy and Whitelaw, 1980; Butler et al., 1980). All of these investigators have either used chemical equilibrium or global Arrhenius expressions to model the flame chemistry. The limitations of such an approach in turbulent environments have been described by Bilger(1977).

Grosshandler and Sawyer(1978) have studied radiation properties of methanol/air combustion products in a test furnace. They have also developed an algorithm for calculating flame radiation(RADCAL). This algorithm is based on the narrow-band model and the Curtis-Godson approximation following Ludwig et al.(1973). Grosshandler and Sawyer(1978) have used measurements of flame structure properties to obtain predictions of radiation intensities. Karman and Steward(1984) have studied the radiation properties of flames burning a mixture of propane and propylene with air. They have reported the enhancement of radiation by adding approximately 7 % by weight(of fuel) of carbon particles to the fuel and air streams. Karman and Steward (1984) have also used measurements of structure properties to obtain encouraging radiation predictions using RADCAL.

Shuen et al.(1986) report a study of an ultra-dilute spray formed by injecting methanol droplets in a methane flame. They state that the droplet concentrations in this study were so small that the flame structure is completely determined by the gaseous methane flame. Radiation properties of the spray flames are not reported but are probably not very different from those of the pure methane flame studied by Jeng and Faeth(1984).

Several papers have addressed the structure and radiation properties of turbulent non-premixed gaseous jet flames (Gore et al., 1987 a,b; Jeng and Faeth, 1984; Gore and Faeth, 1986,1988, Gore, 1988). All of these studies considered single phase gaseous fuels injected into still air. Recently Gore et al.(1988) considered the effects of addition of liquid water into natural gas flames. In practical applications such as spray flames and fires resulting from oil well blowouts, the fuel jet may consist of a two phase mixture. The objective of the present study is to extend the past analysis to the treatment of structure and radiation properties of flames burning two phase mixtures.

A spray of either n-heptane or Alberta sweet crude oil is generated by twin-fluid atomization with part of the methane. The atomization is aided by a coflow of the main methane which also is used to control the mass ratio of the two fuels. Overall heat release rates are nominally 15 MW. Measurements of flame temperatures and radiative heat fluxes to target locations are

obtained.

Theoretical analysis is limited to the locally homogeneous flow (LHF) approximation of multiphase flow theory. Since details of the initial conditions for the present test flames are not precisely known, this is the most logical first step(Faeth, 1988). Even if separated flow calculations are considered, data concerning separate properties of the two phases could not be obtained in the present large scale flames. Within the LHF approximations, flame structure is treated using the conserved scalar formalism and the laminar flamelet concept. State relationships for the present two phase mixture of fuels are not available. Therefore, these are constructed using the state relationships for individual fuels. On the fuel-lean side this amounts to assuming that the two fuels react independently. On the fuel-rich side, there is additional ambiguity concerning the sharing of oxygen between the two fuels.

Once the flame structure is known, the radiation properties are calculated similar to past practice using RADCAL(Grosshandler and Sawyer, 1978). The scattering of radiation by liquid fuel drops is neglected as a first step. In the present analysis, liquid particles can exist only in a small cold interior portion of the spray flame. Therefore, this assumption is consistent.

In the following, the experimental methods and conditions

are summarized. The analysis of flame structure and radiation properties is then described. Finally, results of the experiments and calculations are discussed.

3.2 Experimental Methods

Apparatus

The tests are conducted outdoors since the flame heights are approximately 10 meters. The construction of the burner is similar to the one used by McCaffrey(1986). A twin fluid atomizer (Spraying Systems Inc., model 1J, spray setup 172, fluid nozzle No. 6251000, air cap no. 11251625) is used to inject the liquid fuel (either n-heptane or Alberta sweet crude oil) into a coflow of methane. The coflow tube is 102 mm in diameter with a 50.4 mm diameter 45^{o} sharp-edged orifice plate at the exit. The atomizer assembly is located at a depth of 52 mm from the orifice exit. The coflow of methane is obtained from a "fuel supply tube trailer" which has several 8 meter long commercial gas cylinders in parallel. The main gas flow is metered using an orifice plate and a pressure drop transducer. The gas temperature used in the calculation of the flow rate is measured at the orifice plate using a thermocouple. Atomizing methane gas is obtained from an A1 size commercial gas cylinder. The atomizing gas is metered using a rotameter. Liquid heptane or crude oil is pumped into a vessel and then pressurized using bottled nitrogen. The flow rate of liquid fuels is monitored using a rotameter. The liquid flow

is maintained constant by controlling the pressure in the vessel by adding nitrogen as the liquid level decreases. The burner can be operated for about 5 minutes with the present arrangement.

Instrumentation

Measurements of flame temperatures at five representative locations along the axis of the flames are obtained using type K thermocouples. These are made by joining uncoated 0.5 mm diameter chromel-alumel wires. Steel wires strung between two vertical beams are used to support the thermocouples in the flames. Radiative heat fluxes perpendicular to the axis of the flames are monitored using four water cooled wide angle radiometers (Medtherm Corp., 150^{o} view angle). The radiometers are mounted on a vertical mast at 6.8 meters from the flame axis. A separate radiometer is used to monitor the background radiation since the tests are conducted in an open field. Ambient temperature is also recorded using a thermocouple. The six thermocouple channels, the six radiometer channels, the pressure transducer channel are continuously monitored and stored during the tests using a datalogger and a laboratory computer. Each channel is recorded approximately every five seconds. The ambient wind speed is measured and tests are conducted only when the speed is below 1.0 m/s. Wind speeds of 0.2 to 0.5 m/s are generally observed.

Operating Conditions

Five fully instrumented tests are reported. The test conditions are summarized in Table 1. Three tests involve liquid heptane while two involve Alberta sweet crude oil. The Reynolds numbers at the exit are for both single phase and two phase operation giving fully turbulent flames. The Richardson numbers are low at the injector exit but based on the criteria of Becker and Liang(1978), the flames are affected by buoyancy. A photograph of a typical flame burning the two phase fuel mixture is shown in Figure 10. The flame in Figure 10 appears vertical and symmetric. The visible flame height in Figure 10 is approximately 7 meters. The flames appear to be lifted from the injector exit.

Test Procedure

The tests are started by lighting a small pilot flame of methane . The main and atomizing methane flows are then started and stabilized at the single-phase operating conditions summarized in Table 1 for about one minute. The flow of liquid fuel is then started and stabilized at the two-phase operating conditions for about one minute. Thus during each test, data for a single phase methane flame and a two phase methane+liquid fuel flame are generated.

3.3 Theoretical Methods

The important features of the analysis can be demonstrated

Figure 10. Photograph of a Heptane+Methane Flame.

Table 1: Summary of Test Conditions

Test	$\dot{m}_{CH_4}$[a] Kg/s	$\dot{m}_{liq}$[a] Kg/s	u_o[b,c] m/s	Re[c] $\times 10^{-5}$	Ri[c] $\times 10^{5}$	Q_{CH_4} MW	Q_{Tot} MW
1	0.16	0.22	121	3	3.4	8.0	17.6
2	0.17	0.22	129	3.2	3.0	8.5	18.1
3	0.16	0.22	121	3	3.4	8.0	17.6
4	0.17	0[c]	129	3.2	3.0	8.5	-[d]
5	0.16	0[c]	121	3	3.4	8.0	-[d]

[a] commercial grade_

[b] calculated using actual injector diameter and the total mass flow.

[c] under the present approximation, these quantities are identical for the single-phase and the two-phase flames.

[d] these quantities were not calculated for the

using the pure methane and methane+n-heptane flames due to the relative simplicity of these fuels. Comparative experimental data for the Alberta sweet crude oil is presented without analysis.

Flame Structure

The flame structure analysis is considerably simplified via the locally homogeneous flow approximation(LHF) approach. Under this approximation the multiphase flame reduces to a variable property, single phase reacting flow. Further simplification is achieved when the conserved scalar hypothesis together with the laminar flamelet concept can be utilized. Within these approximations all scalar properties are unique functions of the local instantaneous mixture fraction. The mixture fraction is defined as the fraction of the mass at any location that originated in the fuel stream. Since the density changes substantially, Favre averaging following Jeng and Faeth(1984) is adapted. The effects of liftoff are neglected due to considerable uncertainties in the current understanding (Pitts, 1988).

Within the above approximations, a previously calibrated k-e-g turbulence model is used. Solution of the governing equations for mass, axial momentum and mixture fraction together with the modelled equations for turbulence kinetic energy, dissipation and mixture fraction fluctuations is obtained. All turbulence constants are unchanged from those of Jeng and Faeth(1984). Under the conserved scalar approximation, all instantaneous local

scalar properties are unique functions of the instantaneous local mixture fraction. The specification of these functional relationships (called state relationships by Faeth and Samuelsen, 1986) for two phase mixture of fuels is the main task in the present theoretical work.

Once the state relationships are known, mean values of any scalar property can be found using a probability density function of mixture fraction. Within the present turbulence model only two parameter probability density functions can be treated. Following past practice(Jeng and Faeth, 1984), a clipped Gaussian form is selected.

Initial Conditions

Past laboratory studies have used experimental measurements to specify initial conditions. For the present large scale outdoor flames, this is not feasible due to limitations on resources. The burner design involves injection of a dense spray of liquid in a coflow of gas and subsequent passage of the mixture through a contraction. For the LHF analysis, velocity, density and diameter of a jet equivalent to the conditions produced by the apparatus are needed. This is accomplished by conserving mass and momentum of the incoming streams(Gore et al., 1986). The density of the two phase mixture is calculated by noting that volumes of the phases are additive.

State Relationships

An important task for the present work is the specification of state relationships for the LHF analysis of the two-phase, two-fuel flames. Measurements of species concentrations for n-heptane flames stabilized around porous spheres by Abdel-Khalik et al.(1975) are plotted as a function of local mixture fraction by Bilger(1977) to show that conserved scalar approximation is valid. Therefore, appropriate state relationships for liquid fuels is not an issue in the single phase portions of the spray flame. Measurements of state relationships for fuel rich conditions, which may contain liquid n-heptane, are not available. Faeth(1988) states that these conditions generally involve passive mixing and therefore can be evaluated by simple mixing calculations applied to the relatively lean data. Mao et al.(1980) have demonstrated this approach for a pressure atomized n-pentane spray burning in air at 3 MPa. The method involves chemical equilibrium calculations for regions with temperature greater than 1000 K and extension to lower temperatures by frozen mixing calculations.

The next issue to be addressed is the construction of state relationships for a fuel mixture given the measurements for individual fuels. Three possibilities exist: (1) Conduct measurements of species concentrations in laminar flames burning the fuel mixture under consideration; (2) Following Mao et al.(1980), use chemical equilibrium calculations together with

frozen mixing. However, the choice of the temperature at which the reactions are to be frozen is rather arbitrary; (3) Devise mixing rules for combining the measurements of species concentrations for the two fuels into state relationships for the mixture. The third option is based on the observation that measurements of concentrations of all major species (except carbon monoxide) for the combustion of three different paraffins; methane and propane(Tsuji and Yamaoka, 1969), methane(Mitchell et al., 1980), and heptane(Abdel-Khalik et al., 1975) can all be expressed in terms of a single state relationship for any paraffin (C_nH_{2n+2}). The failure of such general state relationships for carbon monoxide is not expected to affect the radiation predictions due its minor contribution to the total heat flux. Therefore, in the following, the state relationships for the fuel mixture are constructed using those for pure methane and heptane.

Heptane/Air State Relationships

The measurements of Abdel-Khalik et al.(1975) show that the global chemical reaction for n-heptane burning in air considering major species can be written as:

$$aC_7H_{16}(l) + bO_2 + 3.76bN_2 = x_{CO2}CO_2 + x_{C7H16(l)}C_7H_{16}(l)$$

$$+ x_{C7H16(g)} C_7H_{16}(g) + x_{O2}\ O_2$$

$$+ x_{CH4} CH_4 + x_{C2H2} C_2H_2 + x_{C2H4} C_2H_4 \qquad (7)$$

$$+ x_{N2} N_2 + x_{CO} CO + x_{H2O} H_2O + x_{H2} H_2$$

where the product side contains one mole and x_i represents the mole fraction of species "i". Water vapor and hydrogen are not given by Abdel-Khalik et al.(1975) but are calculated using O/N and C/H ratios. Due to their experimental arrangement Abdel-Khalik et al.(1975) did not have any liquid heptane in their measurements. In the present calculations liquid heptane is included to obtain state relationships useful for spray calculations. "a" and "b" on the reactant side are to be calculated using atom balances. The additional unknown in equation (7) is the liquid phase mole fraction of heptane. This is evaluated using the vapor pressure relationship given by:

$$\frac{x_{C7H16(g)}}{(1-x_{C7H16(l)})} = P_v(T) \qquad (8)$$

In order to use the vapor pressure relationship, the temperature of the products must be known. From the conservation of energy for equation (7):

$$(1-X_r)\sum x_i h^o_{fi\ R} = \sum x_i\ h^o_{fi\ P}\ (1-X_r) + \sum x_i \Delta h_{i\ P} \qquad (9)$$

X_r is the radiative heat loss fraction. Similar to past practice a global radiative heat loss fraction is used for all points in the flame(Gore et al., 1986, 1987a, b). Thus each point in the flame loses a fixed fraction of its chemical energy release by radiation. Within this approximation both X_r and the resulting state relationships are independent of the radiative properties (such as optical depth) of the flame.

An auxiliary experiment using 50 mm. and 75 mm. diameter pool flames was completed to obtain the global radiative heat loss fraction for heptane. Total radiative heat fluxes surrounding these flames were measured using a wide angle radiometer and integrated over an envelope to obtain the energy radiated to the surroundings. The chemical energy release was estimated using the liquid consumption rate and the lower heating value of heptane. The resulting X_r of 26 % is used for the heptane state relationships.

Once equations (7)-(9) are solved, the density can be calculated. For the gas phase, the ideal gas law with atmospheric pressure is used to evaluate the density. For the liquid, the density is only a weak function of temperature in the range at which liquid can exist under the LHF approximation. Therefore, a constant density at room temperature is assumed. The density for the two phase mixture is calculated noting that the volumes of the two phases are additive.

Methane/Air State Relationships

Gore et al.(1986) have reported measurements of state relationships for natural gas(predominantly methane)/air flames. These are used here to approximate the methane/air combustion. The measurements of major gas species concentrations can be summarized as:

$$K*(eCH_4 + gO_2 + 3.76gN_2 = x_{CO2*}\ CO_2 + x_{CO*}\ CO + x_{H2O*}H_2O + x_{N2*}\ N_2 + x_{O2*}\ O_2 + x_{H2*}\ H_2 + x_{CH4*}\ CH_4) \quad (10)$$

Where the product side for the equation inside the parenthesis contains one mole and "e" and "g" are found from atom balances. The multiplication factor K for the whole equation is inserted in order to match the mass ratio of the two fuels in creating state relations for the fuel mixture. There is no possibility of liquid in the products of the present system. Therefore, the temperature and density are evaluated by applying equations (9) and the ideal gas law to each of the measurements represented by equation (10).

State Relationships for the Two Phase Fuel Mixture

For simplicity, we assume that the chemical reactions for a mixture of fuels proceed independent of each other. The

individual state relationships for the two fuels (equations (7) and (10)) are to be combined to obtain the state relationships for fuel mixtures. The ratio of the two fuels in the inlet stream is fixed. This ratio must remain unchanged through the mixing and reaction processes for a mixture state relationship to exist. Therefore from equations (7) and (10):

$$16\ Ke/\ 100\ a = R \qquad (11)$$

where "R" is the ratio of mass of methane in the mixture to the mass of heptane. Equations (7) and (11) are sets containing as many individual equations as we choose to obtain from measurements. In order to add individual equations, we need to establish correspondence or decide how oxygen is shared by the two fuels. As a first step we start by assuming that individual equations in the sets equation (7) and equation (11) correspond to each other when their mixture fractions are identical:

$$\frac{100\ a}{(100a + b(28 * 3.76 + 32))} = \frac{16e}{(16e + g(28*3.76 + 32))} \qquad (12)$$

Equations (7), (9)-(12) complete the present approximate rule for construction of state relationships for a mixture given those of the individual fuels.

This procedure corresponds to an implicit assumption that the air is shared by the two fuels in the ratio of their mass. This is only an approximate but a logical first step. Another possibility is that the air is shared in the ratio of the moles of the two fuels. In this case a much leaner methane reaction must be added to a particular heptane reaction. However, any particular mixing rule of this nature for the state relationships is only approximate and must be verified experimentally.

In addition to the concentrations of the gaseous species, soot concentrations for methane+heptane flames are needed. Past spectral radiation intensity data(Jeng and Faeth, 1984; Gore et al., 1986) for methane flames have shown that the contribution of radiation from soot is negligible. Therefore, it is assumed that the continuum radiation from the methane+heptane flames arises from the soot particles produced by the combustion of heptane. Within the Rayleigh approximations, the only quantities needed for determining the absorption coefficient of soot are its volume fraction and refractive index. The refractive index is obtained from Dalzell and Sarofim(1969). Since measurements of soot volume fractions for the present flames are not available, data from Kent(1987) and Olson et al.(1985) for pure heptane are used to estimate the state relationship for the mixture. The calculation involves simple frozen mixing of the products of heptane with those of methane to calculate a new soot volume fraction assuming that the density of the soot particles remains

unchanged. The shape of the state relationship profile for soot volume fractions is assumed to be triangular with a frozen soot region in fuel lean portions similar to that used by Gore and Faeth(1988).

Measurements of X_r for methane+heptane flames are not available. Therefore, an approximate value is estimated by averaging the mass-weighted X_r of the individual fuels.

3.4 Results and Discussion

The state relationships calculated using the procedure discussed above are presented first before discussing the turbulent flame experiments.

State relationships for methane are shown in Figure 11. Concentrations of major gaseous species are plotted as a function of local mixture fraction. These state relationships are identical to the ones used by Gore et al.(1986). Mole fractions of all major gas species except water are obtained from measurements. These are shown in Figure 11. The mole fractions of water vapor are calculated by assuming a fixed C/H ratio at all points.

State relationships for liquid heptane burning in air are shown in Figures 12 and 13. Bilger(1977) plotted the state relationships for the gas phase portion. These are extended to

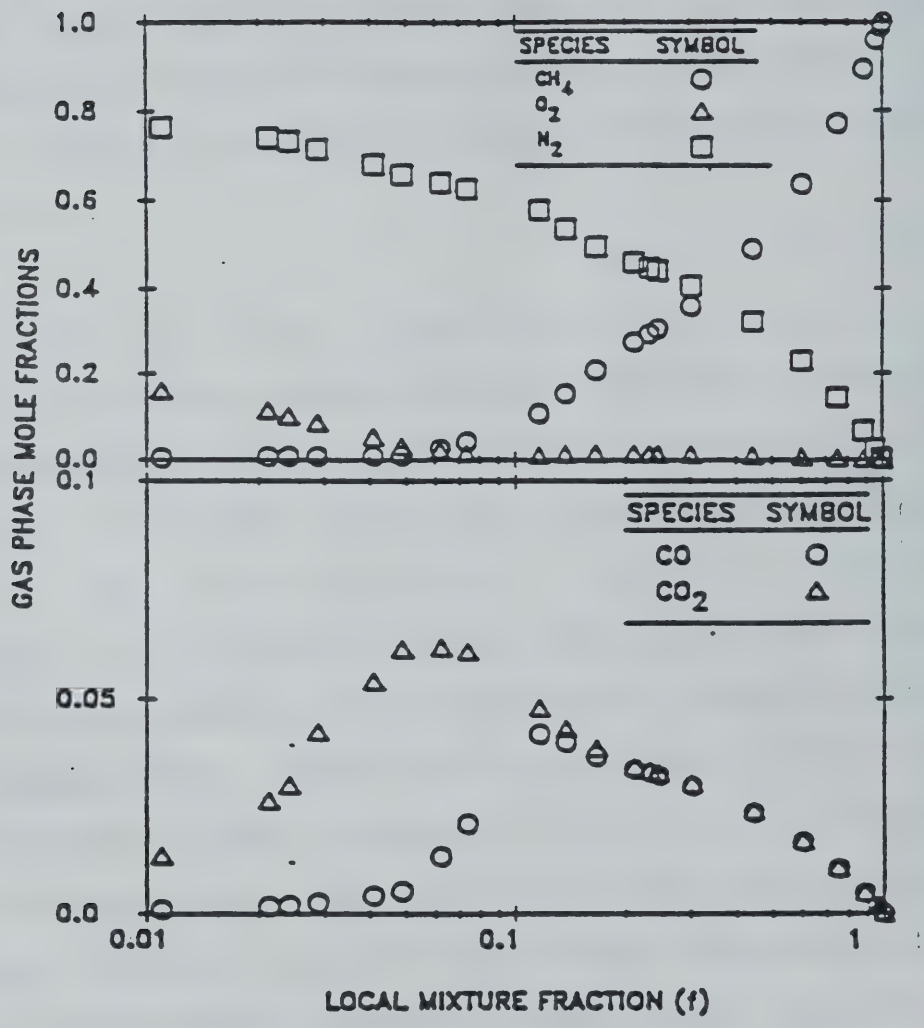

Figure 11. Methane/Air State Relationships.

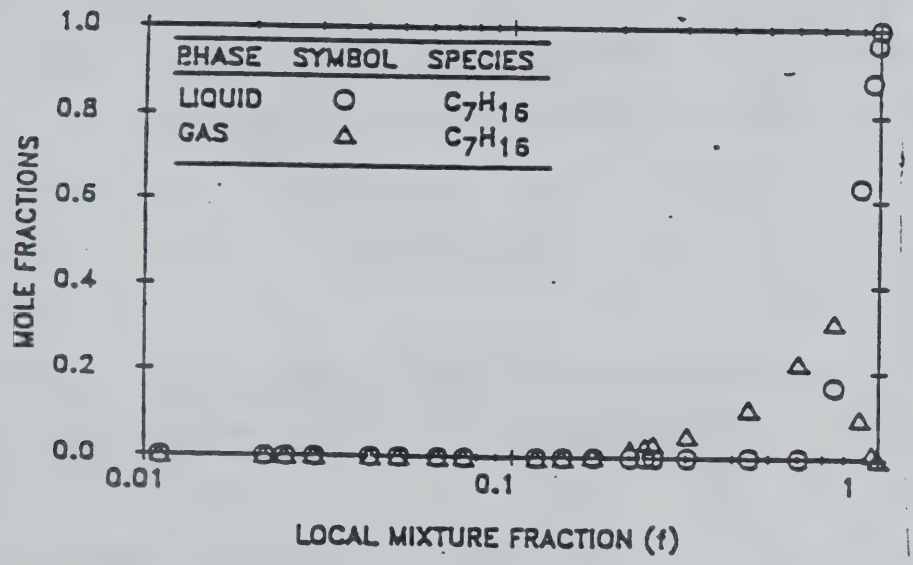

Figure 12. Fuel State Relationships for Heptane/Air Flames.

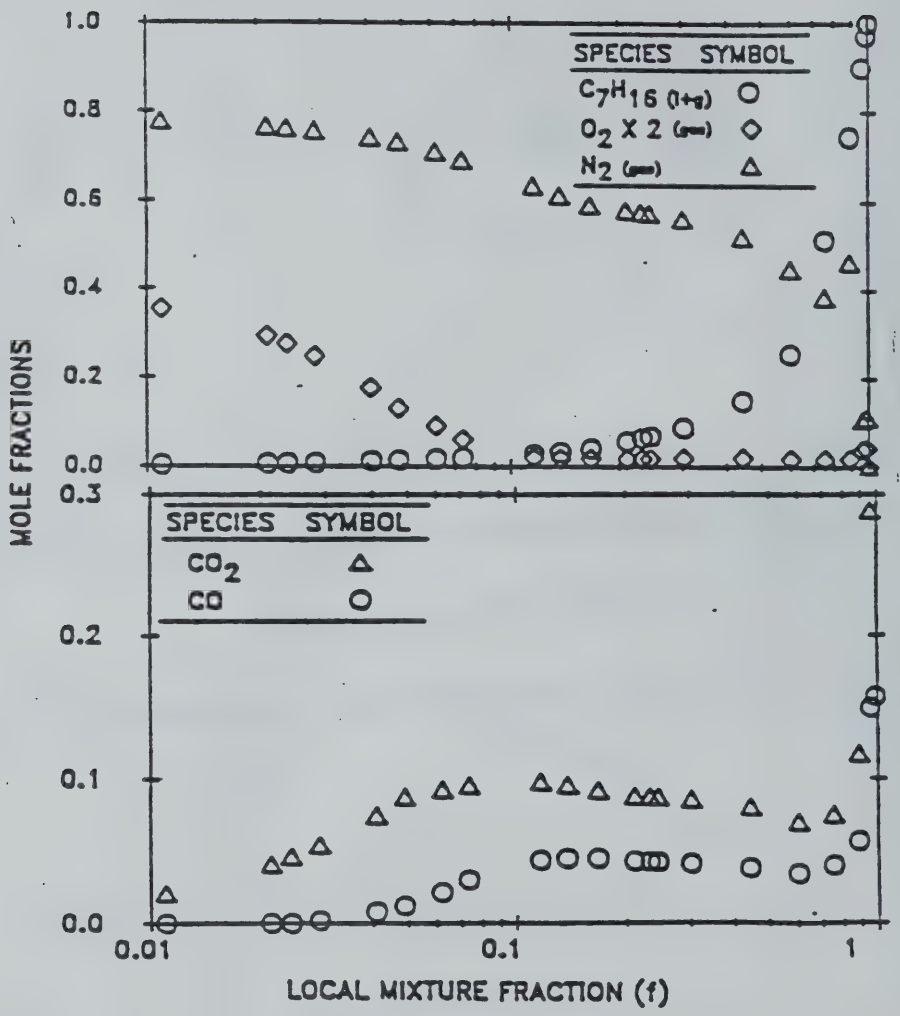

Figure 13. State Relationships for all Species other than Fuel for Heptane/Air Flames.

the liquid-containing region. Mole fractions of liquid heptane and heptane vapor are plotted as a function of mixture fraction in Figure 12. In constructing these state relationships, the measurements are linearly extrapolated to the fuel rich side to obtain the concentrations of heptane(liquid and vapor) and other gas species in the products. Equations (8) and (9) are then used to obtain the temperature and heptane-vapor concentration in the gas phase. The remaining heptane is in the liquid phase. Figure 12 shows that, the concentration of liquid heptane decreases very rapidly. All liquid vanishes at a mixture fraction of 0.6 due to fast transport between the two phases.

Figure 13 shows the state relationships for major gaseous species for heptane used in the present calculation. The mole fractions of all species except heptane are based on the gas phase only. Mole fractions of liquid+vapor heptane are plotted as reference. The mole fractions of gas species increase in regions containing liquid because the total moles in the gas phase decreases.

Figure 14 shows the state relationships for major gas species for a mixture of heptane and methane used in the present experiments(Table 1). These state relationships are obtained by combining those in Figures 11-13 using the mixing rule given by equations (11) and (12) together with the chemical equations (7) and (10). In the inlet fuel stream the mole fraction of liquid

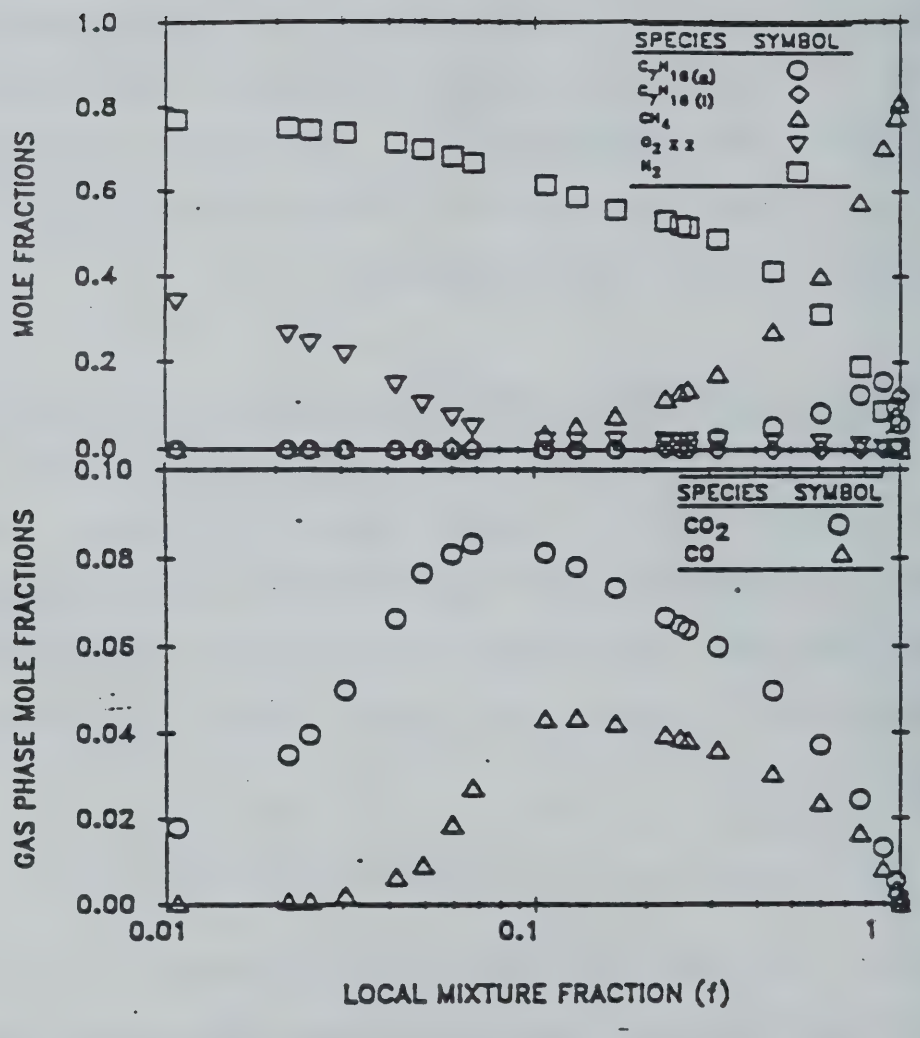

Figure 14. State Relationships for Mixture of Methane + Heptane burning with Air.

heptane is approximately 14%. This liquid rapidly evaporates due to the additional energy release of the gaseous fuel. In fact for the present conditions, all of the liquid fuel evaporates at a mixture fraction of 0.95 as compared to 0.6 for pure heptane. Heptane vapor increases from 0 to approximately 12 percent and then decreases due to pyrolysis and burnout. The mole fractions of CO and CO_2 for the mixture are higher than those for pure methane but lower than those for heptane. For paraffins this is expected due to the increase in the C/H ratio as the order increases.

Figure 15 shows the state relationships for temperatures for methane, heptane and the mixture of the two fuels. The stoichiometric mixture fraction for methane is lower than that for heptane leading to a peak temperature at relatively lower mixture fraction. The temperature levels for methane are higher due to: lower radiation fraction, gas phase at inlet conditions, and higher combustion efficiency. The peak temperature for methane occurs at a mixture fraction close to stoichiometry while for heptane the peak occurs on the fuel rich side. The estimates

of temperatures for the pure heptane flames are lower than the measurements of Abdel-Khalik et al.(1975) by about 350 K. This discrepancy is partly due to the higher radiative heat loss fractions for the present flames in comparison with the droplet flames considered in the previous study. Calculations of flame temperatures using equation (9) are also sensitive to changes in

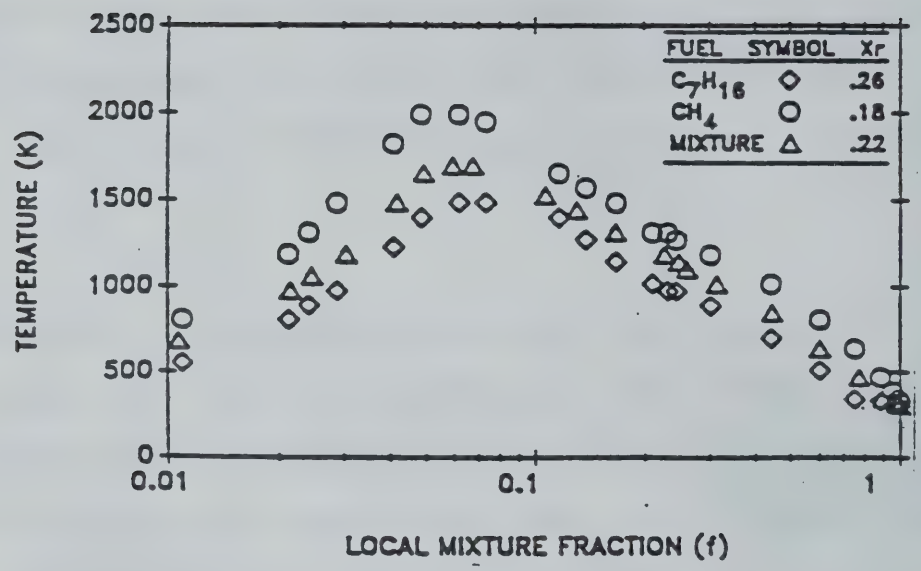

Figure 15. Temperature State Relationships for Heptane/Methane Flames.

the concentrations of species such as CO_2, CO, H_2O and C_7H_{16}.

Above a mixture fraction of 0.6, the temperature for pure heptane is held relatively low by the vaporization of the liquid fuel. As soon as all the liquid evaporates, the temperature begins to rise. The peak value attained is lower than if heptane vapor were injected into the jet. Within the present approximations, the effects of vaporization of liquid on the temperature profile in the fuel rich region of the mixture flames is small.

The turbulent flame experiments involved heptane or crude oil burning with methane. The heptane tests are conducted to simulate oil well blowouts with a simpler fuel. Measurements of temperature profiles and radiative heat fluxes for both flames are discussed in the following. Predictions for the heptane+methane flames are also summarized.

Turbulent Flames

As discussed above, temperature profiles and radiation measurements for flames burning natural gas alone are obtained during the first part of the tests. Since the operating conditions of the five tests during the first minute are almost identical(to the resolution of present instruments and analysis),

these data are grouped together. The five two-phase tests summarized in Table 1 are divided into two groups for the purpose of this discussion. Tests 1-3 form the first group. These involved heptane and methane burning under at almost identical conditions. Tests 4 and 5 involved Alberta sweet crude oil burning together with methane at almost identical operating conditions. These form the second group.

Methane Flames

Figure 16 shows the measurements and predictions of temperatures along the axis of the methane/air flames. The data are obtained by averaging the temperature readings from all five tests summarized in Table 1. The operating conditions are almost identical to the present approximations. The measurements have not been corrected for radiation from the thermocouple. Due to fluctuations in local flow velocities and temperatures, it is not straightforward to correct measurements in a turbulent environment for nonlinear phenomena such as radiation. The estimated corrections range between 50 to 200 K. The visual observations of the flames show liftoff from the injector exit. Although in the calculations the effects of liftoff are neglected, the predicted temperatures begin to develop at approximately x/d= 10 due to the potential core at the injector exit. The agreement between the measurements and predictions in the region near the injector may be fortuitous or may suggest that the effects of liftoff do not penetrate to the flame axis.

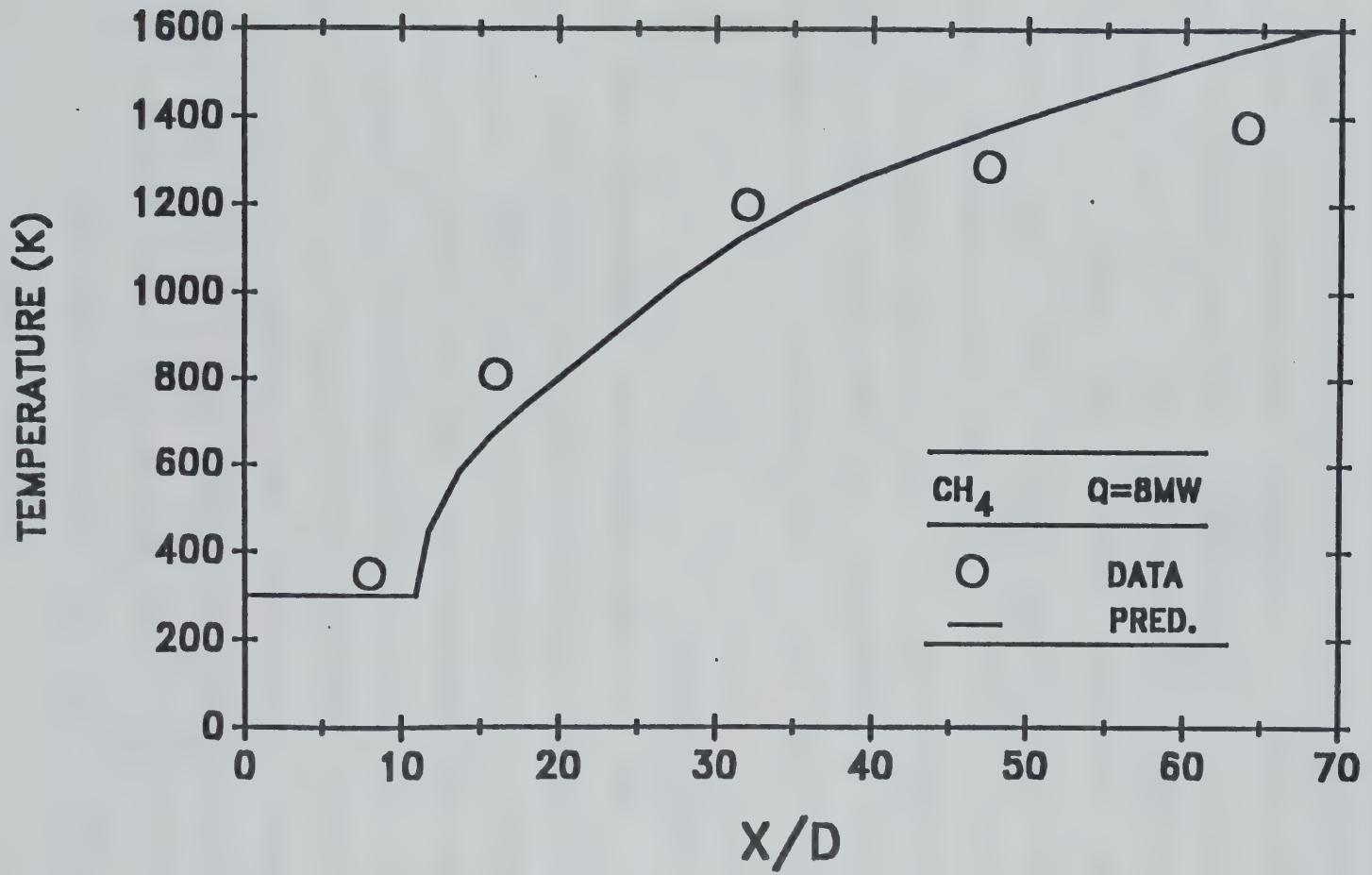

Figure 16. Temperature Profile along the axis of an 8 MW CH_4/Air Flames.

The predicted and measured temperatures are in reasonable agreement similar to past observations(Jeng and Faeth, 1984; Gore et al., 1986, 1988).

Figure 17 shows measurements and predictions of total radiative heat fluxes perpendicular to the axis of the flames at a distance of 6.8 meters. The agreement between measurements and predictions is reasonably good and similar to past findings of Jeng and Faeth(1984) and Gore et al.(1986,1988). Combined with these previous studies, the predictive capabilities of the analyses have been verified for a range of heat release rates between 0.1 MW to 100 MW. Predictions and measurements have compared favorably for heat release rates differing by over four orders of magnitude. All predictions neglected radiation from small quantities of soot particles in the methane flames.

Two Phase Flames

The two phase flames are considered next. Figure 18 shows measurements and predictions of temperatures along the axis of two-phase heptane-methane flames. Data represent averages of tests 1-3. Measurements have not been corrected for radiation transfer from the thermocouples as discussed before. The predicted temperatures are lower by 200 K on an average as compared to the data. The agreement is even worse if radiation corrections are considered. The difference may be due to the high sensitivity of the temperature state relationships to errors in species concentration data discussed earlier.

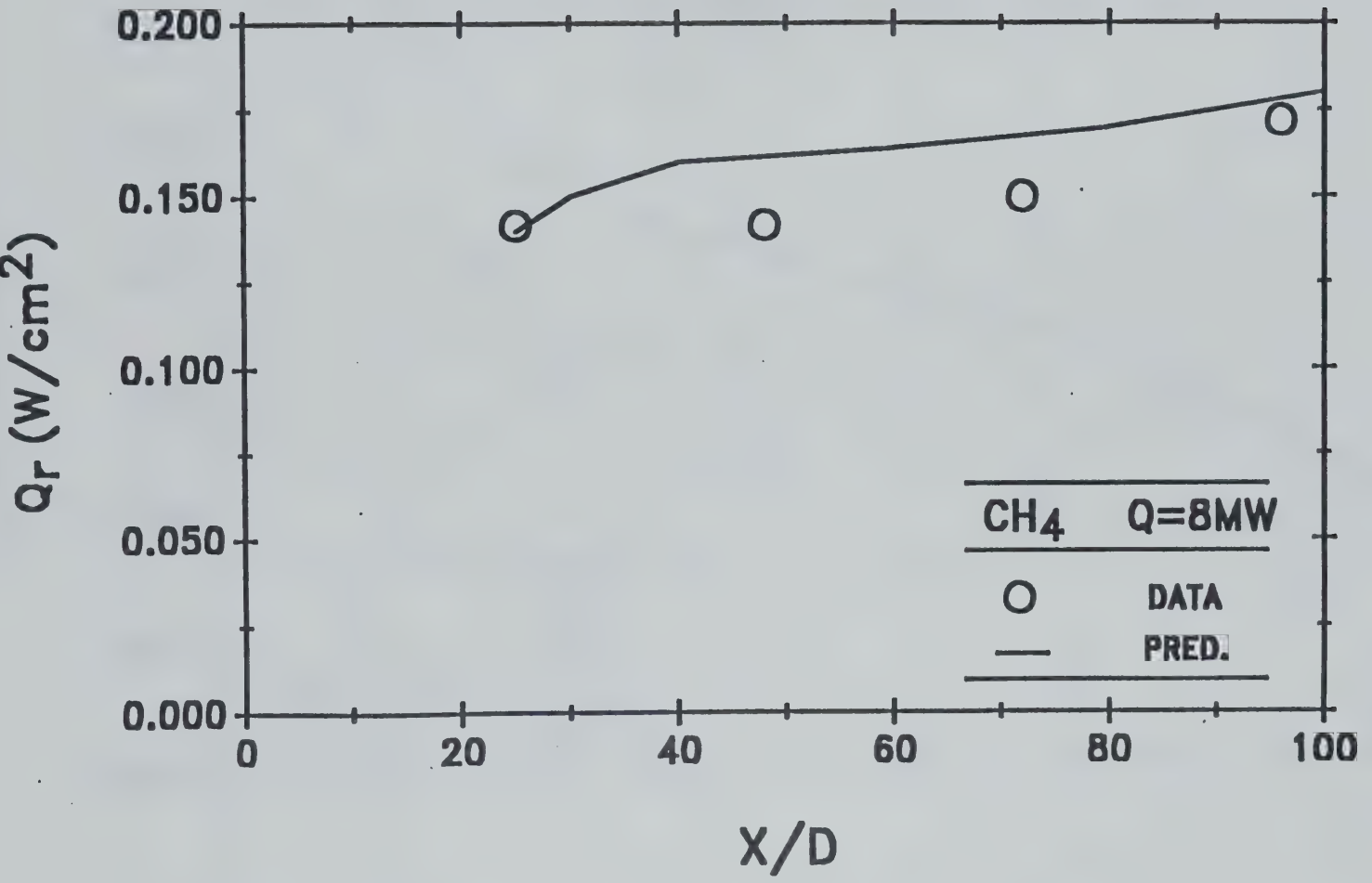

Figure 17. Radiative Heat Fluxes Perpendicular to the Axis of 8 MW CH_4/Air Flames.

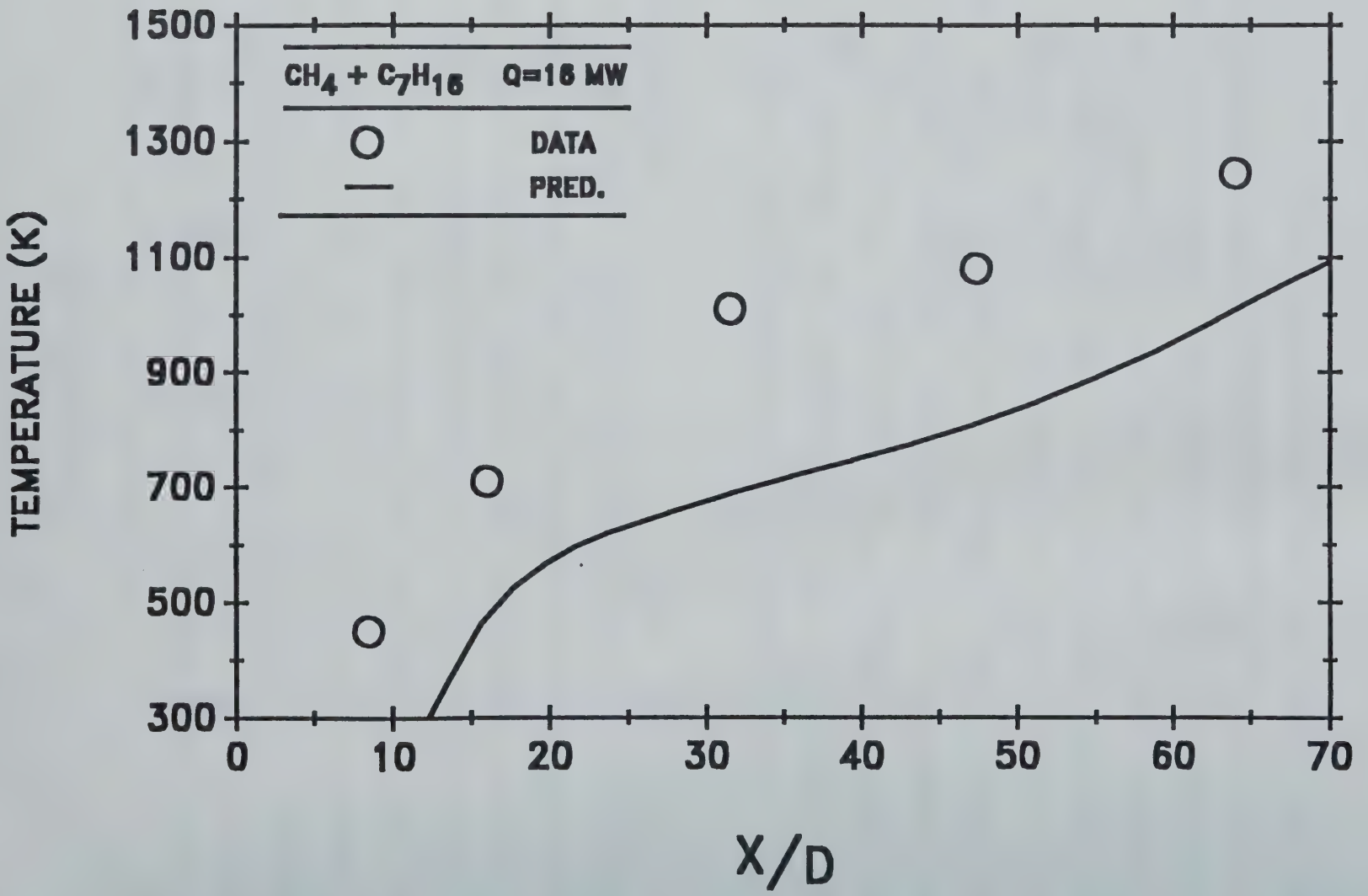

Figure 18. Temperature Profile along the Axis of 16 MW CH_4+C_7H_{16}/Air Flames.

Measurements and predictions of radiative heat fluxes perpendicular to the axis of the two-phase flames are shown in Figure 19. The measured radiation levels are three to six times higher than those for methane flames. Since the heat release rates are almost twice, only a part of this increase is due to the addition of a different fuel(heptane). The analysis underpredicts the radiative heat fluxes by about thirty percent. In addition to the lower estimates of flame temperatures, approximate soot volume fractions could be a reason for this. Turbulence radiation interactions may contribute to the differences as well (Gore and Faeth, 1986, 1988; Gore, 1988). In view of the present approximations, the predictions are encouraging.

Measurements of mean temperatures along the axis and radiative heat fluxes perpendicular to the axis of flames burning Alberta sweet crude oil with methane are used to study the propriety of using heptane to simulate the crude oil in control experiments. Data from tests 4 and 5 are averaged for the purpose of this discussion. Figure 20 shows the distribution of temperatures plotted as a function of normalized distance for the present methane+crude oil flames. The peak temperature levels are similar to those for the methane+heptane flames. The temperature profile for the crude oil flames rises more rapidly suggesting some lower boiling components.

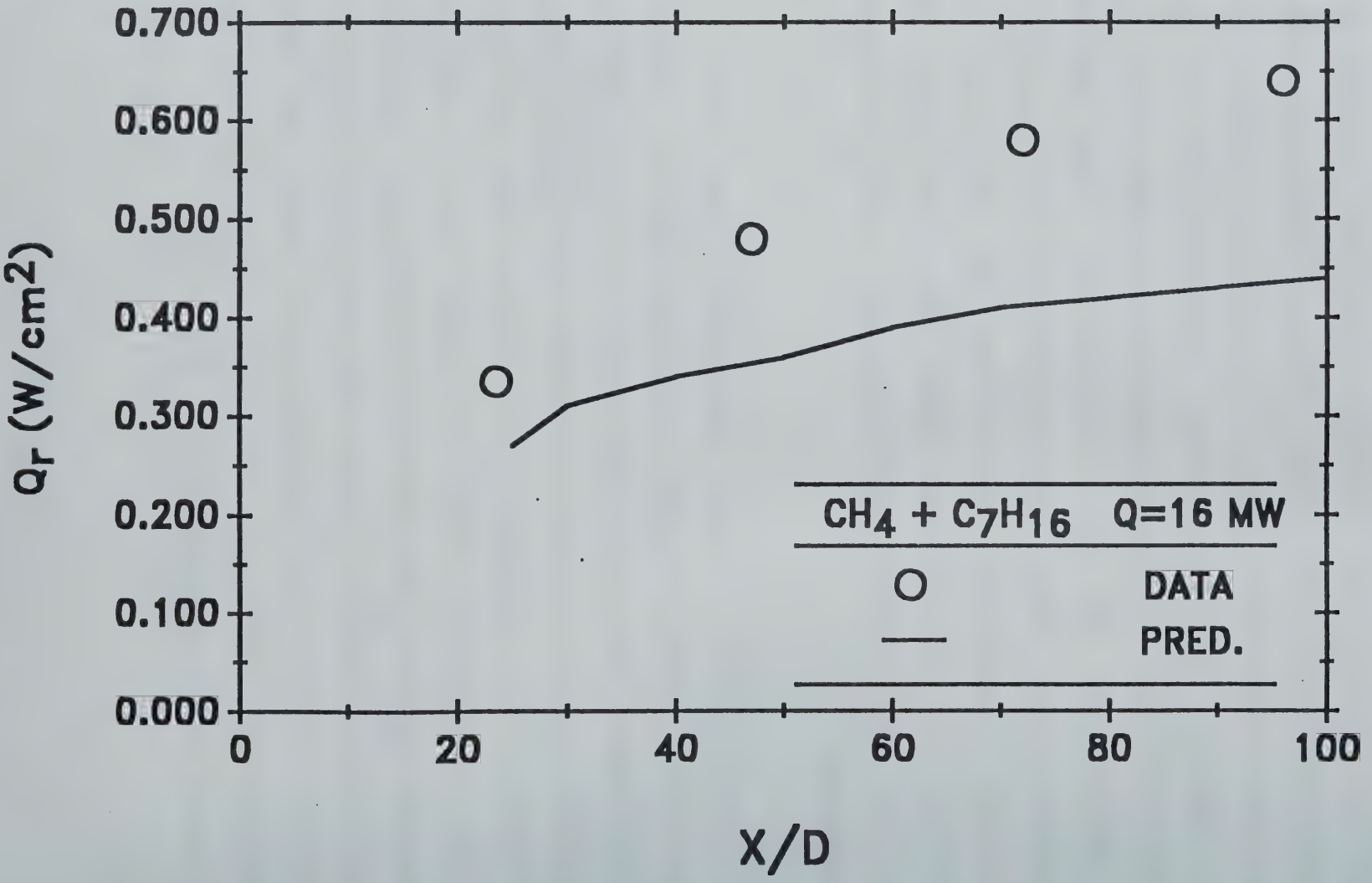

Figure 19. Radiative Heat Fluxes Perpendicular to the Axis of 16 MW CH_4+C_7H_{16}/Air Flames.

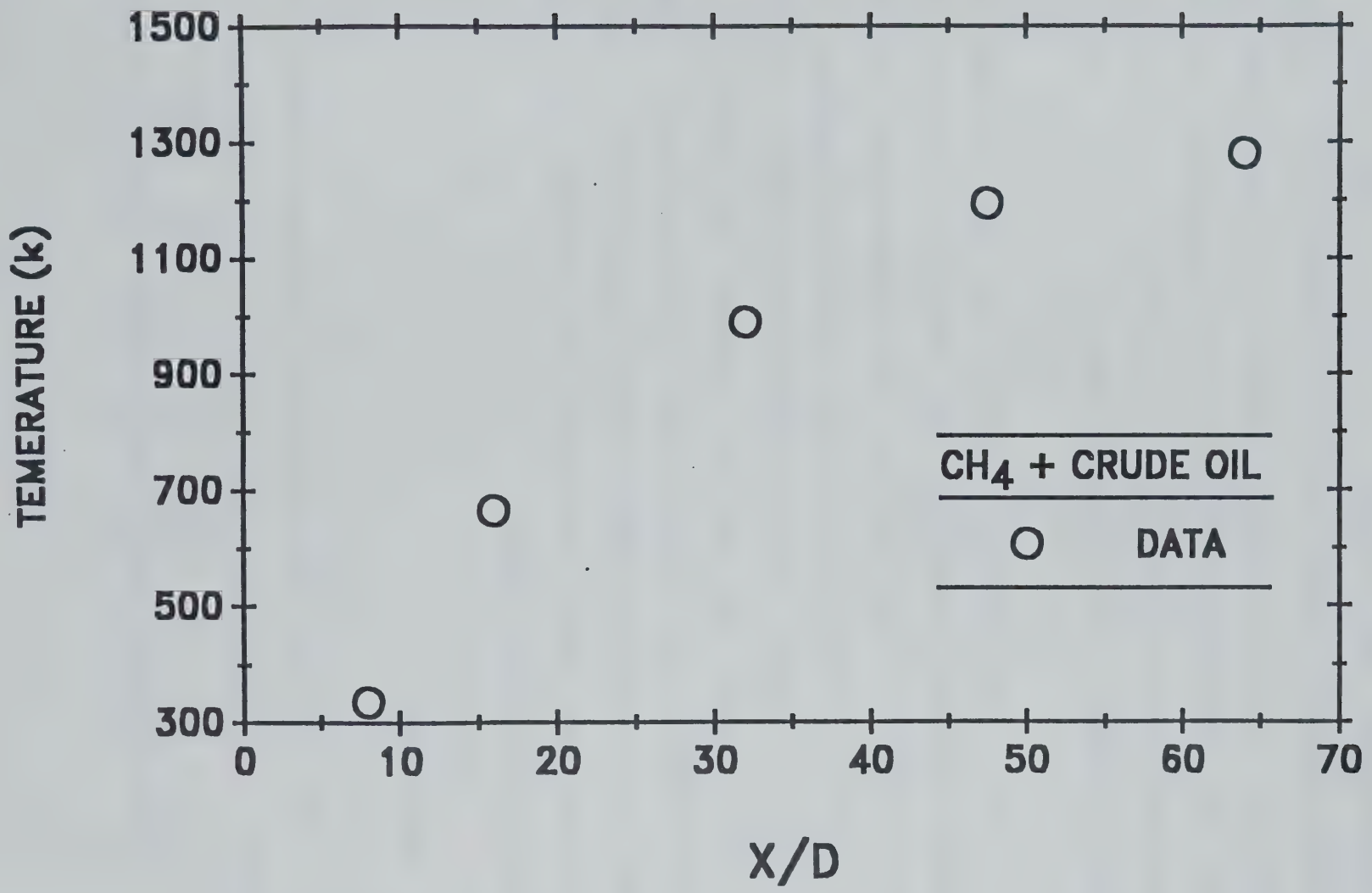

Figure 20. Temperature Profiles along the Axis of CH_4+Alberta Sweet Crude Oil/Air Flames.

Figure 21 shows the measurements of total radiative heat fluxes perpendicular to the axis of the present flames. The peak heat flux levels are three to six times higher than those for methane alone. This increase is similar to that observed for the methane+heptane flames. Near the injector exit, the radiative heat flux levels rise with distance at a faster rate than that seen for heptane+methane flames. This is possibly due to higher suspended solids in the crude oil. Odor of sulfur was certainly noticeable during the crude oil tests.

The temperature levels in the flames burning methane+heptane appear to be comparable to those burning methane+Alberta sweet crude oil as discussed above. If the crude oil flames produce more soot than heptane (as expected), then the reason for similar radiative heat fluxes lies in the different optical depths of the two flames. In particular, self-absorption in the methane+crude oil flames may be higher than that in the methane+heptane flames. Measurements of soot volume fractions and global radiative loss fractions are needed to clarify this issue further.

Conclusions

The following conclusions can be drawn from the present study:

(1) Radiative heat fluxes around present methane air flames are

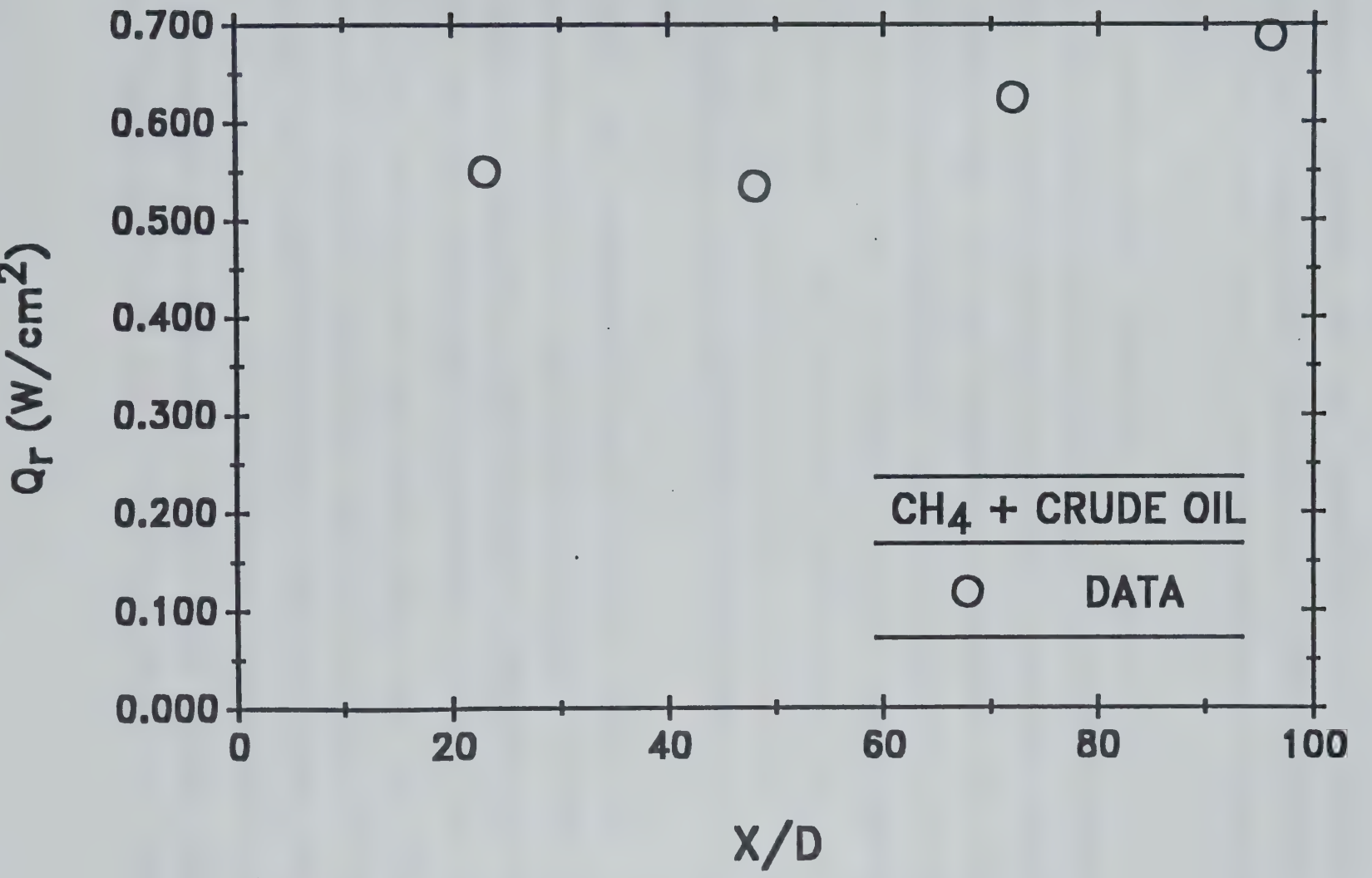

Figure 21. Radiative Heat Fluxes Perpendicular to the Axis of CH_4+Alberta Sweet Crude Oil/Air Flames.

predicted reasonably well, establishing scaleup capabilities of the analysis. However, those around the two-phase flames are underestimated by approximately thirty percent. The reasons include: lower estimates of temperature, complexity of predicting soot in a turbulent environment, and turbulence radiation interactions.

(2) For the present test conditions, heptane appears to be a reasonable choice for simulating Alberta-sweet crude oil in control experiments involving overall radiation properties. The similarity between the radiative fluxes from the two fuels may be due to cancelling effects of radiation emission and self absorption.

4. CO-FLOW BURNER FOR LAMINAR FLAME MEASUREMENTS

The mixing rules for state relationships used in the above two sections are plausible but are not verified by comparison with measurements. Since the kinetic constants of the two fuels and their reaction mechanisms likely to be different, the mixing rules for state relationships must be verified experimentally. For this purpose a laminar coflow burner similar to the one used in the past has been constructed and tested for satisfactory operation. Similar burners have been used by Mitchell et al., 1980; Santoro et al., 1983 and Faeth and coworkers (Gore and Faeth, 1986, 1988, Gore et al. 1986, 1987a and 1987b). Figure 22

shows a sketch of the laminar flame burner constructed for measuring state relationships for fuel mixtures. As a first step two gaseous fuels will be tested to separate the complications of phase change processes. Acetylene, a heavily sooty fuel with complex chemistry is selected as a component with methane which is a relatively clean burning predominant component of oil well blowout efflux.

Preliminary measurements of soot volume fractions using the new burner have been completed and are in agreement with past data. Measurements of gas species concentrations for fuel mixtures will be completed during the upcoming year to test the mixing rules for state relationships. Mixing rules for soot volume fractions will also be examined. Once appropriate mixing rules for state relationships are in place, attention will be focussed on two phase flames representative of oil well blowouts.

REFERENCES

Abdel-Khalik S.I., Tamaru, T. and El-Wakil M.M (1975), "A Chromatographic Study of the Diffusion Flame Around a Simulated Drop," Fifteenth Symposium (International) on Combustion, The Combustion Institute, Pittsburgh, pp. 389-399.

Becker H.A. and Liang D., 1978, "Visible Length of Vertical Free Turbulent Diffusion Flames," Comb. Flame, Vol. 32, pp. 115-137.

Bilger R.W., 1977, "Reaction Rates in Diffusion Flames," Comb. Flame, Vol. 30, pp. 277-284.

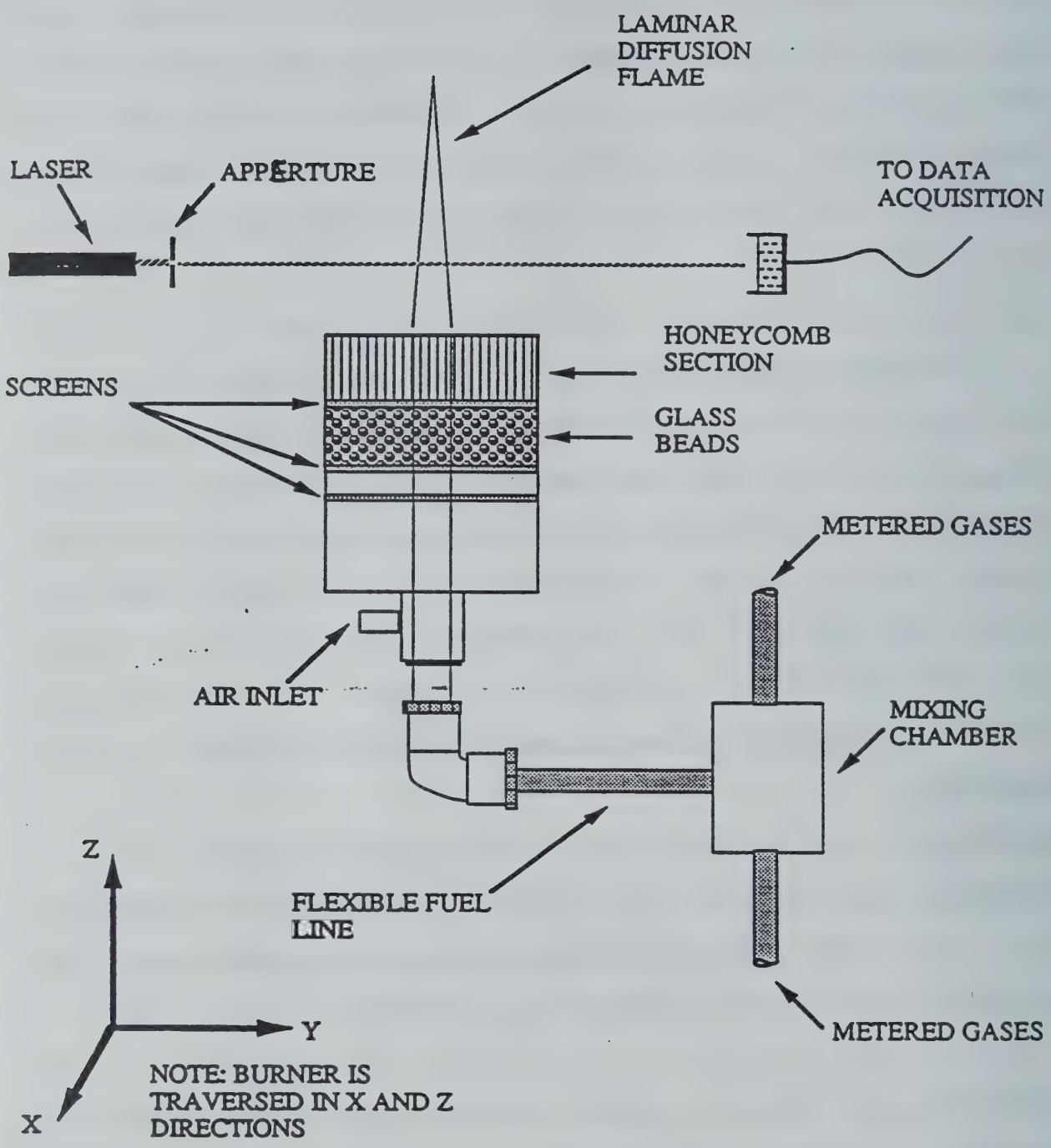

Figure 22. Laminar Coflow Burner for State Relationship Measurements.

Butler T.D., Cloutman L.D., Dukowicz J.K., Ramshaw J.D. and Krieger R. B., 1980, "Toward a Comprehensive Model for Combustion in a Direct-Injection Stratified-Charge Engine," Combustion in Reciprocating Engines, J.N. Mattavi and C.A. Amann, eds., Plenum, New York, pp. 231-264.

Dalzell W. H. and Sarofim A. F., 1969, "Optical Constants of Soot and Their Application to Heat Flux Calculations," J. Heat Trans., Vol. 91, pp. 100-104.

El Banhawy Y. E. and Whitelaw J. H., 1980, "Calculations of the Flow Properties of a Confined Kerosene-Spray Flame," AIAA J., Vol. 18, No. 12, pp. 1503-1510.

Evans D. D. and Pfenning D. B., 1985, "Water sprays suppress gas-well blowout fires," Oil and Gas J., Vol. 83, No. 17, pp. 80-86.

Faeth G.M., 1977, "Current Status of Droplet and Liquid Combustion," Prog. Energy Combust. Sci., Vol. 3, pp. 191-224.

Faeth G.M., 1983, "Evaporation and Combustion of Sprays," ibid, Vol. 9, pp. 1-76.

Faeth G.M., 1988, "Mixing, Transport and Combustion in Sprays," ibid, Vol. 13, pp. 293-345.

Faeth G.M., and Samuelsen G.S., 1986, "Fast Reaction Non-Premixed Combustion," Prog. Energy Combust. Sci., Vol. 12, pp. 305-372.

Gore J.P., 1988, "Coupled Structure and Radiation Analysis of Turbulent Diffusion Flames," Collected Papers in Heat Transfer, 1988, Vol. 2(K.T. Yang ed.), ASME, New York, pp. 77-86.

Gore J.P., Jeng S.M., and Faeth G.M., 1987a, "Spectral and Total Radiation Properties of Turbulent Carbon Monoxide /Air Diffusion Flames," AIAA J., Vol. 25, No. 2, pp. 339-345.

Gore J.P., Jeng S.-M., and Faeth G.M., 1987b, "Spectral and Total Radiation Properties of Turbulent Hydrogen/Air Diffusion Flames," J. Heat Trans., Vol 109, No. 1, pp.165-171.

Gore J.P. and Faeth G.M., 1986, "Structure and Spectral Radiation Properties of Turbulent Ethylene/Air Diffusion Flames," Twenty-First Symposium (International) on Combustion, The Combustion Institute, Pittsburgh, pp. 1521-1531.

Gore J.P. and Faeth G.M., 1988, "Structure and Spectral Radiation Properties of Turbulent Acetylene/Air Diffusion Flames," J. Heat Trans., Vol. 110, No. 1, pp.173-181.

Gore J.P., Faeth G.M., Evans D.D. and Pfenning D.B., 1986, "Structure and Radiation Properties of Large Scale Natural Gas/Air Diffusion Flames," Fire and Materials, Vol. 10, pp. 161-

169.

Gore J.P., Evans D.D and McCaffrey B.J., 1988, " Temperature and Radiation Properties of Large Methane/Air Flames with Water Suppression," Proceedings of the Twenty-First Fall technical Meeting of the Eastern States Section, The Combustion Institute, Pittsburgh, PA., pp. 60.1-60.4.

Gosman A.D. and Ioannides E., 1981, "Aspects of Computer Simulation of Liquid-Fueled Combustors," AIAA Paper No. 81-0323.

Gosman A.D., Ionnides E., Lever D.A. and Cliffe K. A., 1980, "A Comparison of Continuum and Discrete Droplet Finite-Difference Models Used in the Calculation of Spray Combustion in Swirling Turbulent Flows," AERE Harwell Report TP865.

Grosshandler W.L. and Sawyer R.F., 1978, "Radiation from a Methanol Furnace," J. Heat Trans., Vol. 100, pp. 247-252.

Jeng S.M. and Faeth G.M., 1984, "Radiative Heat Fluxes Near Turbulent Buoyant Methane Diffusion Flames," J. Heat Trans., Vol. 106, pp. 886-888.

Karman D. and Steward F.R., 1984, "The Radiation Spectrum of a Test Furnace," Int. J. Heat Mass Trans., Vol. 27, pp. 1357-1364.

Kent J. H., 1987, "Turbulent Diffusion Flame Sooting-Relationship to Smoke Point Tests," Comb. Flame, Vol. 67, pp. 223-233.

Lockwood, F. C., and Shah, N. B., 1981, "A New Radiation Solution Method for Incorporation in General Combustion Prediction Procedures," Eighteenth Symposium (International) on Combustion, The Combustion Institute, Pittsburgh, pp. 1405-1414.

Ludwig C.B., Malkmus W., Reardon J.E. and Thomson J.A., 1973, Handbook of Infrared Radiation From Combustion Gases, NASA SP-3080.

Mao C.P., Szekely G.A. and Faeth G.M., 1980, "Evaluation of a Locally Homogeneous Model of Spray Combustion," J. Energy, Vol. 4, pp. 78-87.

McCaffrey, B.J., 1986, "Momentum Diffusion Flame Characteristics and the Effects of Water Spray," NBSIR 86-3442, National Institute of Standards and Technology, Gaithersburg, MD., also Combust. Sci. and Tech., Vol. 63, pp. 315-335, 1989.

McCaffrey, B. J., 1984, "Momentum Diffusion Flame Characteristics and the Effects of Water Sprays," Combust. Sci. and Tech., Vol. 40, pp. 107-136.

McCaffrey B. J. and Evans D. D., 1986, "Very Large Methane Jet

Diffusion Flames," Twenty First Symposium (International) on Combustion, The Combustion Institute, Pittsburgh, PA, pp. 25-31.

Mitchell R.E., Sarofim A.F. and Clomberg L.A., 1980, "Experimental and Numerical Investigation of Confined Laminar Diffusion Flames," Comb. Flame, Vol. 37, pp. 227-234.

Mongia H.C. and Smith K., 1978,"An Empirical/Analytical Design Methodology for Gas Turbine Combustors," AIAA Paper No. 78-998.

Olson D.B., Pickens J.C. and Gill R.J., 1985, "The Effects of Molecular Structure on Soot Formation II Diffusion Flames," Comb. Flame, Vol. 62, 43-60.

Pfenning D. B., 1985, "Blowout Fire Simulation Tests, NBS-GCR-85-484, Final Report by Energy Analysts Inc., Norman, OK., to U. S. Dept. of Commerce.

Pitts W. M., 1988, "Assessment of Theories for the behavior and Blowout of Lifted Turbulent Jet Diffusion Flames," Twenty Second Symposium (International) on Combustion, The Combustion Institute, Pittsburgh, PA., pp. 809-816.

Santoro R. J., Semerjian H. B. and Dobbins R. A., 1983, "Soot Particle Measurements in Diffusion Flames," Comb. Flame, Vol. 51, pp. 203-218.

Seshadri, K., 1978, "Structure and Extinction of Laminar Diffusion Flames Above Condensed Fuels with Water and Nitrogen," Comb. Flame, Vol. 33, pp. 197-215.

Shuen J.S., Solomon, A.S.P. and Faeth G.M., 1986, "Drop-Turbulence Interactions in a Diffusion Flame," AIAA J., Vol. 24, No. 1, pp. 101-108.

Spalding D.B., 1977, GENMIX: A General Computer Program for Two-Dimensional Parabolic Phenomena, Pergamon Press, Oxford.

Swithenbank J., Turan A. and Felton P.G., 1980, "Three-Dimensional Two-Phase Mathematical Modelling of Gas Turbine Combustors," Gas Turbine Combustor Design Problems, A. H. Lefebvre ed., Hemisphere, Washington, pp. 249-314.

Tsuji, H. and Yamaoka, I., 1969, " The Structure of Counterflow Diffusion Flames in the Forward Stagnation Region of a Porous Cylinder," Twelfth Symposium (International) on Combustion, The Combustion Institute, Pittsburgh, PA, pp. 997-1005.

NIST-114A
(REV. 3-90)

U.S. DEPARTMENT OF COMMERCE
NATIONAL INSTITUTE OF STANDARDS AND TECHNOLOGY

BIBLIOGRAPHIC DATA SHEET

1. PUBLICATION OR REPORT NUMBER
NIST-GCR-90-581

2. PERFORMING ORGANIZATION REPORT NUMBER

3. PUBLICATION DATE
November 1990

4. TITLE AND SUBTITLE

An Investigation of Simulated Oil-Well Blowout Fires

5. AUTHOR(S)

J.P. Gore, S.M. Skinner and U.S. Ip

6. PERFORMING ORGANIZATION (IF JOINT OR OTHER THAN NIST, SEE INSTRUCTIONS)

University of Maryland
Mechanical Engineering Department
College Park, MD 20742

7. CONTRACT/GRANT NUMBER
Grant No. 60NANB8D0834

8. TYPE OF REPORT AND PERIOD COVERED
Annual Report September 1989

9. SPONSORING ORGANIZATION NAME AND COMPLETE ADDRESS (STREET, CITY, STATE, ZIP)

U.S. DEPARTMENT OF COMMERCE
National Institute of Standards
and Technology
Gaithersburg, MD 20899

10. SUPPLEMENTARY NOTES

11. ABSTRACT (A 200-WORD OR LESS FACTUAL SUMMARY OF MOST SIGNIFICANT INFORMATION. IF DOCUMENT INCLUDES A SIGNIFICANT BIBLIOGRAPHY OR LITERATURE SURVEY, MENTION IT HERE.)

A study of simulated oil well blowout fires aimed at improving predictive capabilities needed for the development of radiation and fire suppression technology is described. Measurements of temperature distributions and radiative heat flux to representative locations are used to evaluate the analysis. Methane/air flames with suppression and heptane+methane/air flames without suppression are considered. The analysis consists of (i) construction of state relationships for fuel with water addition and two phase fuel mixtures using species concentration data for single fuels with the help of mixing rules and (ii) application of an existing flow solver under the locally homogeneous flow approximation. The predictions and measurements are in reasonably good agreement. Direct verification of the mixing rule for state relationships and treatment of two phase flow effects is necessary for further improvement.

12. KEY WORDS (6 TO 12 ENTRIES; ALPHABETICAL ORDER; CAPITALIZE ONLY PROPER NAMES; AND SEPARATE KEY WORDS BY SEMICOLONS)

blowout fires; fire investigations; fire suppression; flame radiation; flame structure; heat flux; laminar flames; oils; simulation; temperature measurements; water; well fires

13. AVAILABILITY

[X] UNLIMITED

[ ] FOR OFFICIAL DISTRIBUTION. DO NOT RELEASE TO NATIONAL TECHNICAL INFORMATION SERVICE (NTIS).

[ ] ORDER FROM SUPERINTENDENT OF DOCUMENTS, U.S. GOVERNMENT PRINTING OFFICE, WASHINGTON, DC 20402.

[X] ORDER FROM NATIONAL TECHNICAL INFORMATION SERVICE (NTIS), SPRINGFIELD, VA 22161.

14. NUMBER OF PRINTED PAGES
81

15. PRICE
A05

ELECTRONIC FORM